NASA Contractor Report 4367

Superplastic Formability of Al-Cu-Li Alloy Weldalite™ 049

Bao-Tong Ma and Joseph R. Pickens

CONTRACT NAS1-18531
MAY 1991

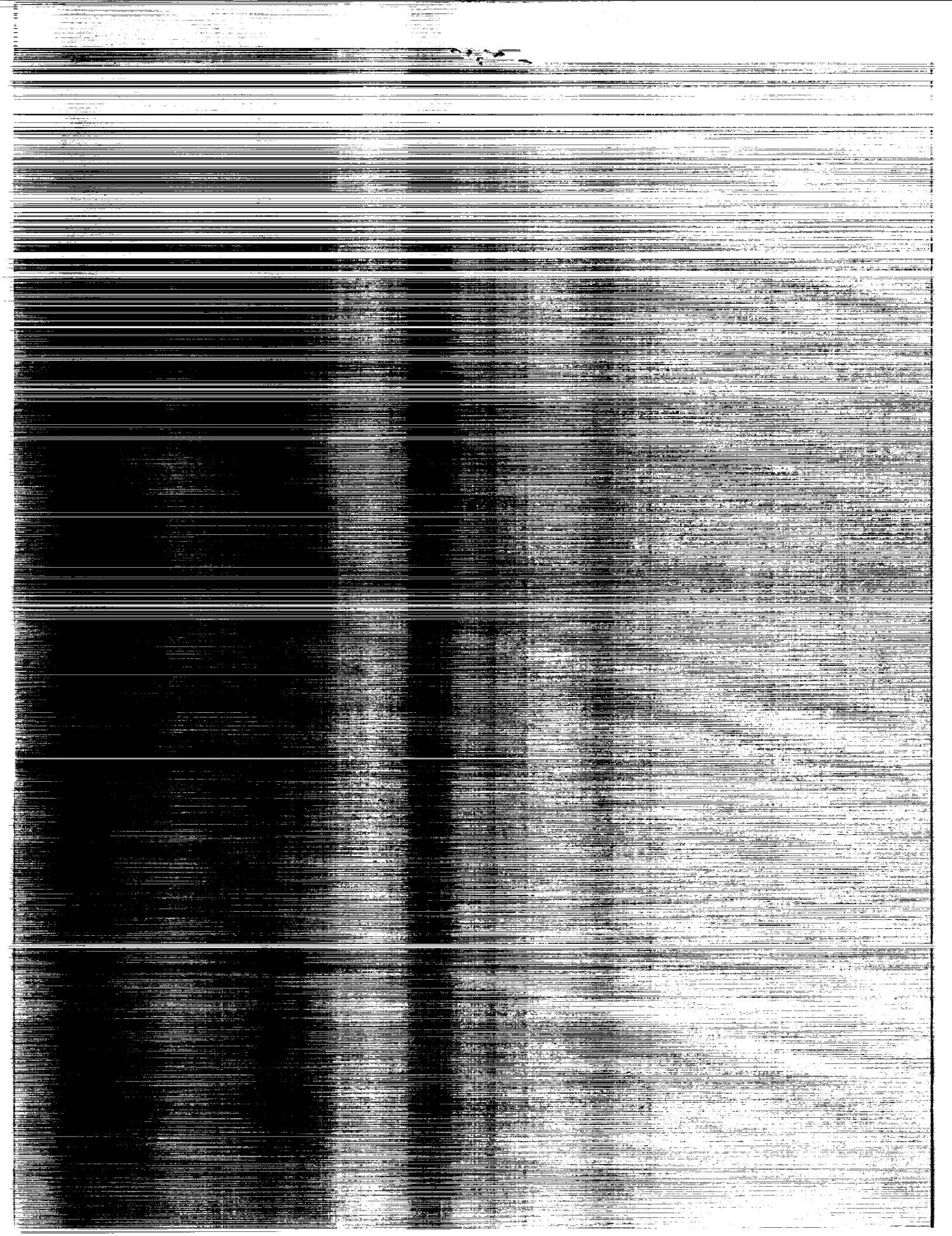

NASA Contractor Report 4367

Superplastic Formability of Al-Cu-Li Alloy Weldalite™ 049

Bao-Tong Ma and Joseph R. Pickens
Martin Marietta Corporation
Martin Marietta Laboratories
Baltimore, Maryland

Prepared for
Langley Research Center
under Contract NAS1-18531

National Aeronautics and
Space Administration
Office of Management
Scientific and Technical
Information Division

1991

ABSTRACT

Extensive research during the past decade shows that several aluminum lithium alloys can be processed to attain a microstructure that enables superplasticity. The high tensile strength of Al-Cu-Li alloy Weldalite™ 049 in the T4 and T6 tempers offers tremendous potential for attaining exceptional post-SPF properties. The SPF material used in this study is Weldalite™ 049 sheet that has been processed by Reynolds Metals Company's proprietary technique, which has been shown to induce SPF behavior in other Al-Cu-Li alloys. Martin Marietta Laboratories has evaluated the superplastic behavior and resulting post-SPF mechanical properties of this alloy, which was designed to be the next major structural alloy for space applications. The results indicate that Weldalite™ 049 alloy does indeed exhibit excellent superplasticity over a wide range of temperatures and strain rates and excellent post-SPF tensile strength at various potential service temperatures.

ACKNOWLEDGEMENTS

The authors thank Frank H. Heubaum at Martin Marietta Laboratories, Roy Crooks at the Rockwell International Science Center, Bill James at NASA Langley Research Center and Joe Terrell at Reynolds Metal Company for their experienced help in this work. We are especially grateful to William Brewer, contract monitor, for his critical review of this manuscript and his patience during the early stages of the program.

TABLE OF CONTENTS

List of Tables

List of Figures

1.0 INTRODUCTION

Superplastic forming (SPF) has emerged as an important manufacturing process for reducing the fabrication costs associated with aerospace structural systems. It can decrease machining costs by providing net shape components and also reduce costs associated with fastening. Innovative joining technologies used in conjunction with a superplastically formed structure can significantly reduce the cost of an aerospace structure component and can potentially improve its damage tolerance. It is significant that most components made by SPF are not amenable to subsequent uniform introduction of cold work. For Al-Cu and Al-Cu-Li alloys, uniform cold work (i.e., T8 temper) is needed to attain the highest strength, because dislocations are needed to stimulate the nucleation of strengthening precipitates. Consequently, SPF parts made from Al-Cu and Al-Cu-Li alloys are often used in the non-cold worked, artificially aged (T6) temper.

In most cases of SPF, the microstructure of an alloy is modified by thermomechanical processing (TMP) to obtain an array of fine, equiaxed, high-angle grain boundaries that are stabilized by relatively fine dispersoids. The alloy then can deform to large strains at elevated temperatures (e.g., > 50%, the absolute melting-point temperature) when deformed at relatively low strain rates (i.e., 10^{-6} - 10^{-3} s^{-1}). The mechanism of SPF deformation often involves grain boundary sliding with the aforementioned microstructure. Alternatively, the sheet can be warm or cold rolled to produce a highly deformed, unrecrystallized microstructure that exhibits SPF

behavior in subsequent deformation at elevated temperature. In some cases during elevated temperature deformation, dynamic recrystallization occurs, which eliminates the accumulated work thereby allowing very large (e.g. > 300%) strains to be realized.

Weldalite™ 049 was specifically designed to attain ultra-high strength in both naturally and artificially aged tempers without the need for cold work to stimulate precipitation. This is significant because Al-Cu-Li alloys such as 2090 attain low strength in the non-cold worked naturally aged temper (T4), e.g., about 30 ksi, and only moderate strength (62 ksi) in the non-cold worked artificially aged temper (T6). Weldalite™ 049 reproducibly attains ultra-high tensile strength in the T4 (86 ksi) and T6 (> 100 ksi) tempers, which offers tremendous potential for attaining exceptional post-SPF properties.

1.1 Project Objectives

The major objectives of this research were to 1) assess the amenability of Weldalite™ 049 to superplastic formability 2) identify advantageous superplastic forming parameters, 3) fabricate SPF demonstration parts, and 4) evaluate the post-SPF mechanical properties. Although thermomechanical processing schemes were investigated to induce superplasticity in Weldalite™ 049, the major emphasis was placed on assessing Weldalite™ 049 that was processed by Reynolds Metals Company's proprietary technique.

To meet the objectives, both uniaxial and biaxial superplasticity were assessed and the post-SPF mechanical properties of SPF parts were evaluated. Specific items addressed were superplastic elongation, superplastic deformation behavior, strain-rate sensitivity,

activation energy for superplastic flow, various superplastic forming parameters such as temperature, strain rate, back pressure, post-forming pressure, etc., and post-SPF tensile strength.

1.2 Material

Weldalite™ 049 sheet (0.125 inch thick) was provided by Reynolds Metals Company, the commercial producer of Weldalite™ 049 sheet and plate. This material was processed by Reynolds' proprietary thermomechanical technique (TMT) to induce SPF in the alloy. The composition of the as-received SPF-processed Weldalite™ 049 sheet and the nominal Weldalite™ 049 composition are shown in Table I.

TABLE I

Composition (wt%) of Weldalite™ 049 Alloy

	Cu	Li	Ag	Mg	Zr
Nominal	4.75	1.30	0.40	0.40	0.14
Measured	4.70	1.25	0.38	0.37	0.15

2.0 EVALUATION OF UNIAXIAL SUPERPLASTICITY

2.1 Uniaxial Superplastic Elongation

The dimensions of the tensile-test specimens were chosen to be the same as those used by Reynolds (i.e., a gauge length of 0.5 inch long by 0.3 inch wide), so that results could be compared. All of the tests were performed in an MTS servo-hydraulic system at constant crosshead speed without back pressure. Tensile tests were carried out at temperatures of 820, 860, 900, and 940°F in air, at initial strain rates of $8x10^{-3}$, $4x10^{-3}$, $2x10^{-3}$, $1x10^{-3}$, and $6x10^{-4}$ s^{-1}. Applied loads were recorded on an X-Y chart recorder. The temperature was controlled in a three-heat-zone furnace with one controller. A homogeneous temperature distribution throughout the furnace was maintained within an acceptable range (plus or minus 3°F) during the period of the tensile test.

Superplastic elongations of Weldalite™ 049 were obtained without back pressure over a technologically useful range of deformation temperatures and strain rates as shown in Table II. The results are very encouraging and indicate that Weldalite™ 049, as processed by Reynolds' proprietary technique, does indeed exhibit excellent superplasticity. For example, the best SPF elongation, 931%, was obtained at a temperature near 900°F and an initial strain rate of $1x10^{-3}$ s^{-1} (see Table II). A superplastic elongation of 560% or more can be obtained over a wide temperature and strain-rate range, as indicated by the area within the triangle in Table II.

TABLE II

Superplastic Elongation of Weldalite™ 049 without Back Pressure

Initial Strain Rate (s^{-1})	Testing Temperature (°F) SPF Elongation (%)			
	820	860	900	940
$8x10^{-3}$	286	317	404	465
$4x10^{-3}$	294	396	436	829
$2x10^{-3}$	319	358	650	791
$1x10^{-3}$	420	710	813 931*	618
$6x10^{-4}$	560	>892	803	671

*A superplastic elongation of 931% was obtained at a strain rate of $1x10^{-3}$ s^{-1} and an unknown temperature. Although the testing temperature was originally set at 820°F, the actual temperature was higher and was estimated to be between 880°F and 920°F.

The results also show that good superplasticity can be attained at a relatively high strain rate: for example, a superplastic elongation of 829% was obtained at a strain rate of $4x10^{-3}$ s^{-1} at 940°F. This is the solution-heat-treatment temperature for Weldalite™ 049 and the high SPF elongation at that temperature has particular technological significance, because it offers the possibility of quenching the alloy directly from the forming temperature to attain high strength in the T4 and T6 tempers without a subsequent solution treatment.

2.2 Deformation Behavior in Hot Tensile Tests at Constant Crosshead Speed

The deformation behavior of a superplastic material in a constant-crosshead-speed test is quite different from that in a constant-strain-rate test. For example, most superplastic materials tested at constant strain rate experience a steady-state flow stress, where the flow stress increases rapidly at an early stage of deformation due to work-hardening, and then remains nearly constant throughout most of the ensuing superplastic elongation. However, when a superplastic material is tested at constant crosshead speed, the strain rate decreases as the specimen elongates and the measured flow stress does not reach a steady state.

Figure 1 shows a typical load-displacement curve for Weldalite™ 049 in a constant-crosshead-speed test at a superplastic temperature of 860°F. True stress vs superplastic elongation curves can be generated from these data if constant volume and uniform deformation along the gage length of the specimen are assumed. Such

Fig. 1. Load-displacement curve for superplastic Weldalite™ 049, tested at 860°F and an initial strain rate of 4×10^{-3} s^{-1}.

stress-elongation curves, shown in Fig. 2 for various deformation temperatures and strain rates, are characterized by their peaks. The flow stress increases rapidly during the work-hardening stage, as in a constant-strain-rate test, but drops dramatically with elongation as soon as its maximum value is reached. The maximum stress is attained at an elongation of about 80%, independent of deformation temperature and strain rate, but the magnitude of the maximum stress depends on deformation temperature and initial strain rate. The higher the temperature, or the lower the initial strain rate, the smaller the maximum stress. Therefore, a superplastic material tested at constant crosshead speed exhibits a unique value of maximum stress under specific conditions of temperature and strain rate. This maximum flow stress is frequently used for other analyses, for example, in evaluating strain-rate sensitivity, calculating activation energy, estimating gas pressure profiles for superplastic forming, etc. The variation of the maximum flow stress with testing temperature and initial strain rate is shown in Table III.

Based on the peaks of the flow stress vs. elongation curves, the curves can be divided into two regions: Region I, a region of work-hardening, which covers elongations up to 80%; and Region II, a region where the measured flow stress decreases with elongation sharply up to 400% elongation, and then slows down. The dramatic decrease of the flow stress in Region II is likely in part related to the decrease of strain rate with elongation that occurs in tensile tests performed at constant crosshead speed. Because superplastic materials, such as Weldalite™ 049, are highly sensitive to the strain rate, such a variation in strain rate will greatly affect the magnitude

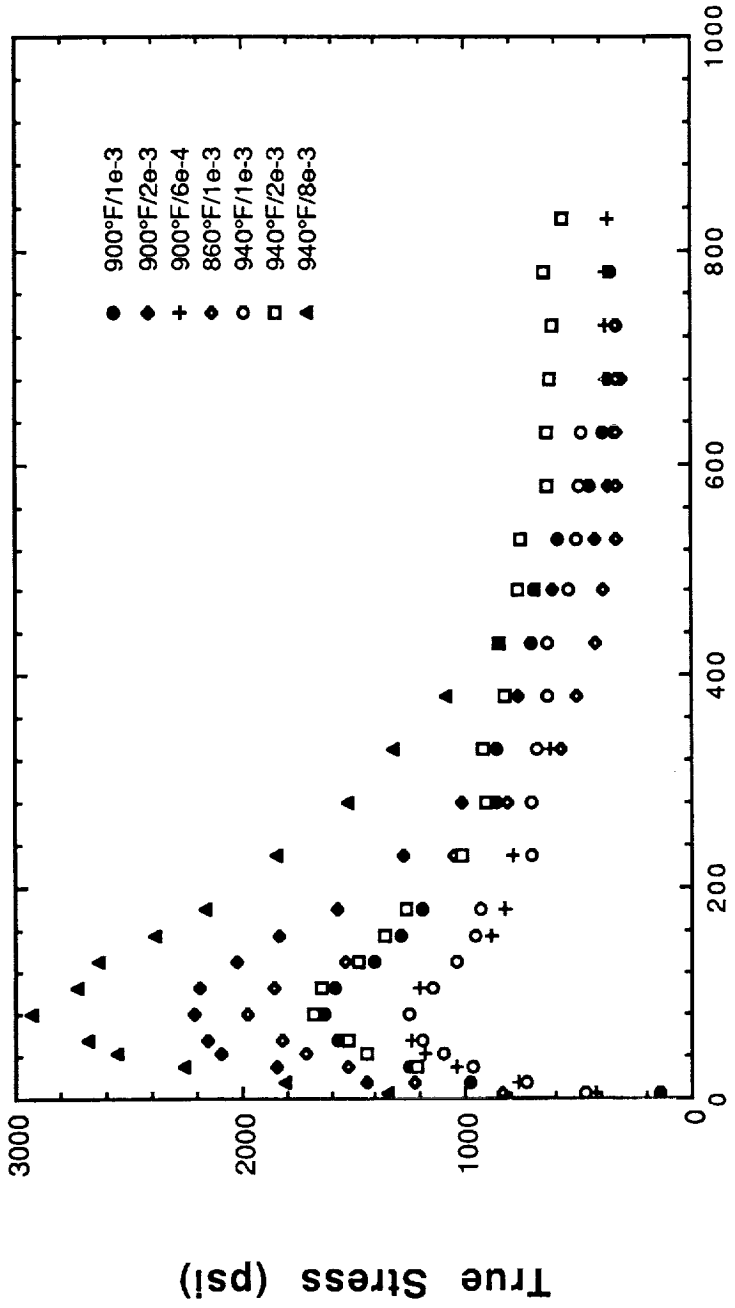

Fig. 2. The true stress vs superplastic elongation for Weldalite™ 049, tested at various temperatures and initial strain rates.

TABLE III

Maximum True Flow Stress of Weldalite™ 049 in SPF Tensile Tests at Constant-Crosshead-Speed

Initial Strain Rate (s^{-1})	Testing Temperature (°F) 820	860	900	940
	Maximum True Flow Stress (ksi)			
$8x10^{-3}$	5.4	4.4	3.5	2.9
$4x10^{-3}$	4.6	3.7	2.7	2.2
$2x10^{-3}$	3.4	2.5	2.2	1.6
$1x10^{-3}$	2.9	2.0	1.6	1.2
$6x10^{-4}$	2.3	1.8	1.2	0.9

of the flow stress. The relationship between the flow stress and the strain rate is shown in Fig. 3 which is a plot of true flow stress and true strain rate vs superplastic elongation. It can be seen that flow stress decreases with decreasing strain rate, suggesting that the decrease in strain rate is a major contribution to the decrease of the flow stress in Region II of the constant cross-head speed tests.

2.3 Strain-Rate Sensitivity

The theoretical strain-rate sensitivity, m, of a material is defined as:

$$\sigma = K\dot{\varepsilon}^{m} \qquad (1)$$

or

$$m = \frac{\partial \ln(\sigma)}{\partial \ln(\dot{\varepsilon})} \qquad (2)$$

where σ and $\dot{\varepsilon}$ are the flow stress and the strain rate, respectively, and K is a material constant. In an ideal material, where the microstructure remains unchanged during deformation, the true flow stress can be determined from measurements of the steady-state load at each rate applied during constant strain-rate tests. Then, the m value can be calculated based on the relationship between applied strain rate and the true flow stress. However, because of the experimental difficulties of obtaining low or constant strain rates in conventional tensile testing equipment, most m values are obtained

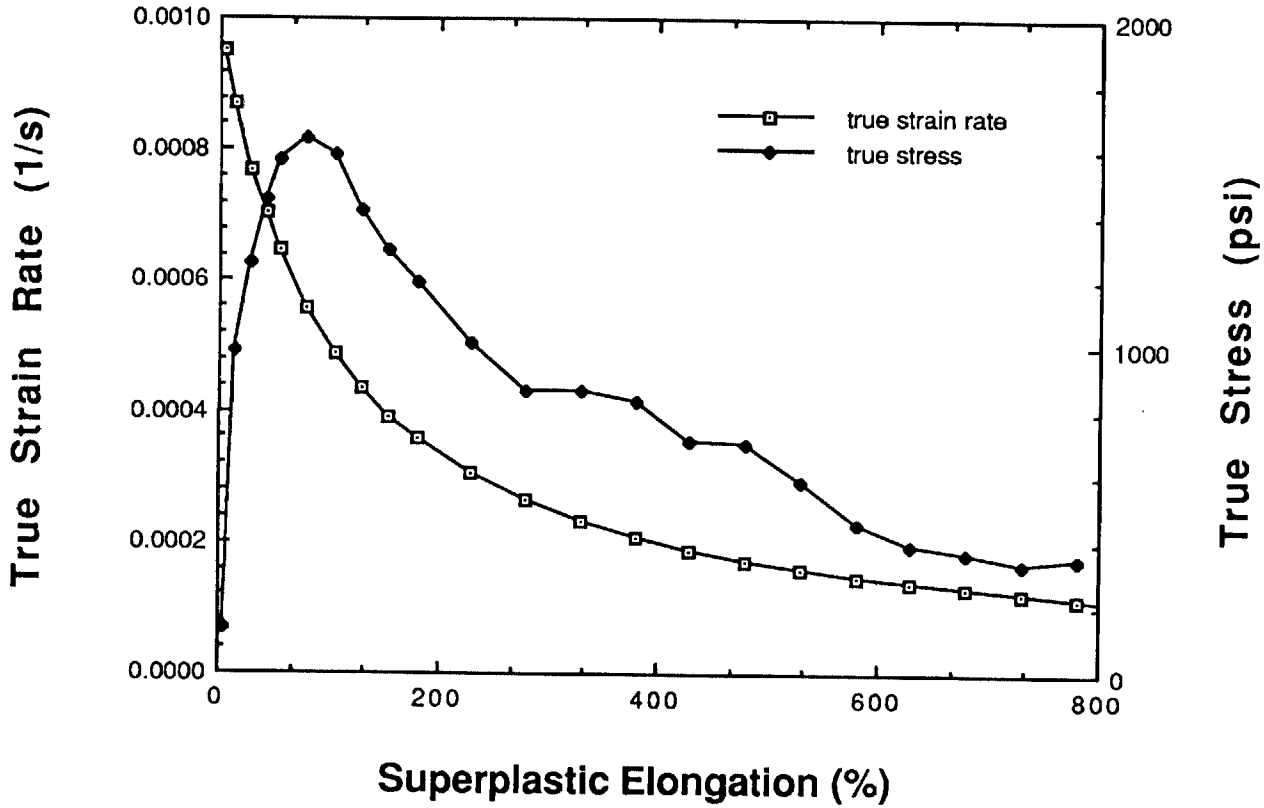

Fig. 3. The variation of strain rate and true stress with superplastic elongation for Weldalite™ 049, tested at 900°F and an initial strain rate of $1x10^{-3}$ s^{-1}.

from stepped strain-rate tests or stepped crosshead-speed tests. Therefore, real-world strain-rate sensitivity is often defined as:

$$m = \frac{\Delta \ln(\sigma)}{\Delta \ln(\dot{\varepsilon})} = \frac{\ln(\sigma_1/\sigma_2)}{\ln(\dot{\varepsilon}_1/\dot{\varepsilon}_2)} \qquad (3)$$

where σ_1 and σ_2 are the values for steady state true stress at constant or instantaneous strain rates $\dot{\varepsilon}_1$ and $\dot{\varepsilon}_2$, respectively.

It is clear that the m values derived from Eqs. (2) and (3) will differ, because most assessments of superplasticity and strain rate sensitivity are obtained from constant-crosshead-speed tests rather than constant-strain-rate tests. During constant-crosshead-speed tests, the true strain rate decreases as the specimen elongates; thus, all else being equal, the flow stress decreases with increasing strain as mentioned above, and the m value further deviates from its theoretical definition [Eq. (2)].

The m value of Weldalite™ 049 was evaluated via a series of stepped constant-crosshead-speed tests at 900°F over the strain range where Weldalite™ 049 might be expected to exhibit superplastic behavior. Since many engineering materials do not have a uniform initial structure, a certain amount of strain was allowed to accumulate before the crosshead speed was changed. The strain rate sensitivity and its variation with strain rate were determined from the true flow stress and instantaneous strain rate at each crosshead speed. The true flow stress was calculated from the steady-state load at each speed (measured from an X-Y chart recorder) and the cross-sectional area of the specimen (calculated from the instantaneous

gage length of the specimen, assuming both constant volume and a uniform cross-sectional area).

The data obtained from the load-vs-elongation record for specimens deformed at 900°F are summarized in Table IV, together with the calculated values of true stress and true strain rate. A logarithmic plot of true stress vs true strain rate is shown in Fig. 4. The strain-rate sensitivity at a given strain rate can be determined either by constructing tangents to the curve or by evaluating the derivative of the polynomial expression defining the curve. We chose the former. The variation of the m value with strain rate, obtained by calculating tangents to the curve shown in Fig. 4, is plotted in Fig. 5. The peak value of m in excess of 0.5 is obtained at the strain-rate range between $2x10^{-4}$ and $1x10^{-3}$ s^{-1}, where the greater superplastic elongations (about 800%) are also observed. Superplastic elongations (more than 300%) are obtained in the strain-rate range between $2x10^{-5}$ and $4x10^{-3}$ s^{-1} where m is greater than 0.3, the approximate threshold typically observed for SPF behavior.

2.4 Activation Energy for Superplastic Flow

Plastic flow, especially at elevated temperature, is a thermally activated process. Experimental evaluation of the activation energy, Q, of plastic deformation and its dependence on stress, temperature, deformation, strain rate, etc., is an effective way of determining the validity of theoretical models for dislocation processes in solids. Macroscopic tension-test measurements of the temperature and

TABLE IV

Load, Elongation, and True Stress and Strain Rate for Weldalite™ 049 from Stepped Constant Crosshead-Speed Tests at 900°F

Crosshead Speed (in./s)	Initial Strain Rate (1/s)	Running Time (s)	Specimen Length (in.)	True Strain Rate (1/s)	True Cross-Sectional Area (in^2)	Load (lb)	True Stress (psi)
-	-		0.5		0.0375		
$5x10^{-3}$	10^{-2}	100	1.00	$5x10^{-3}$	0.0188	45	2400
$5x10^{-4}$	10^{-3}	500	1.25	$6.7x10^{-4}$	0.0150	17	1133
$5x10^{-5}$	10^{-4}	1000	1.30	$9.1x10^{-5}$	0.0144	8	555
$2.5x10^{-6}$	$5x10^{-5}$	1000	1.325	$4.8x10^{-5}$	0.0142	5.5	389
$5x10^{-6}$	10^{-5}	500	1.330	$1.0x10^{-6}$	0.0141	4	284

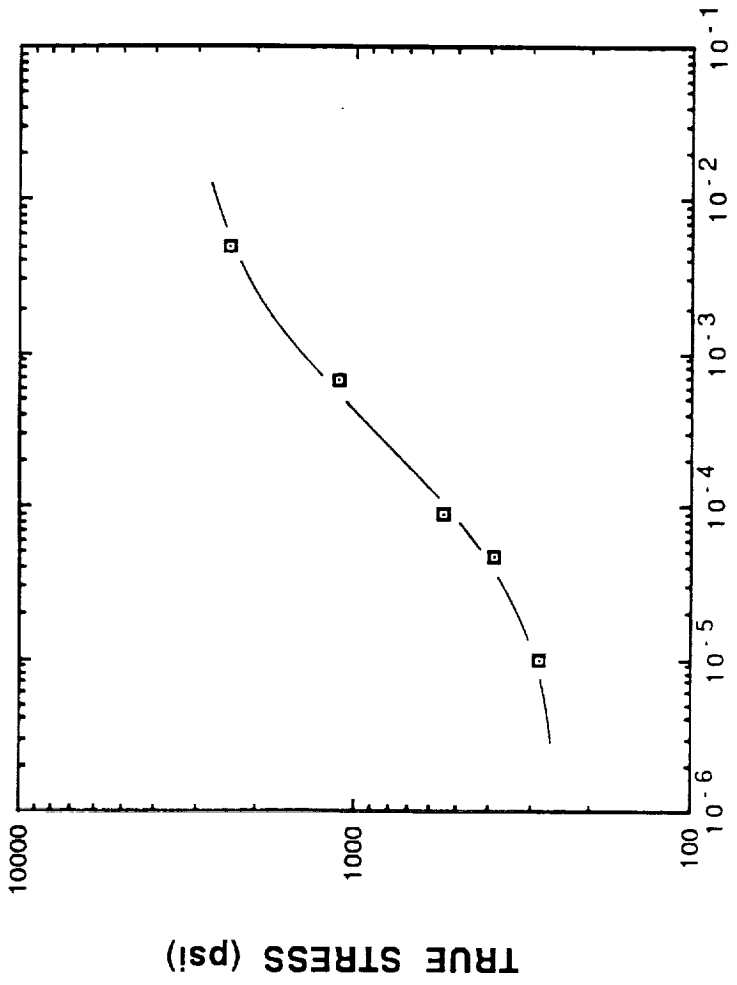

Fig. 4. The relationship between the true stress and the true strain rate obtained in a stepped strain-rate test.

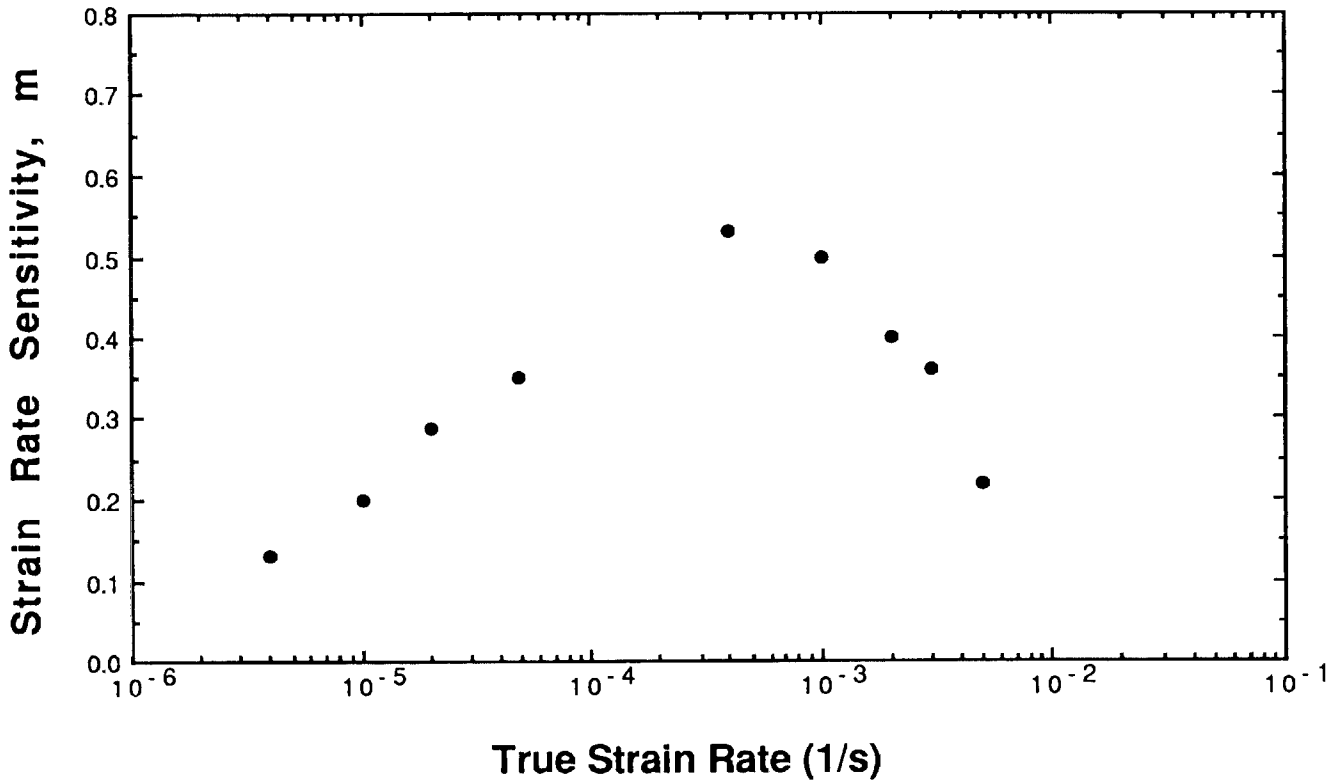

Fig. 5. The variation of the strain rate sensitivity, m, with strain rate obtained by calculating tangents to the true stress vs strain rate curve shown in Fig. 4.

strain-rate dependence of flow stress provide direct insight into possible dislocation behavior in the superplastic deformation of Weldalite™ 049.

In order to evaluate the activation energy for superplastic flow of Weldalite™ 049, a few assumptions are necessary. First, it is assumed that the flow stress of Weldalite™ 049 deformed at superplastic deformation temperatures obeys the creep power law, $\sigma=K\dot{\varepsilon}^m$, or:

$$\dot{\varepsilon} = A\exp(-Q/RT)\sigma^{1/m} \qquad (4)$$

which can be rewritten as

$$\ln(\dot{\varepsilon}) = B + 1/m\ln(\sigma) - Q/RT \qquad (5)$$

where A and B are material constants, and R and T represent the gas constant and the absolute temperature, respectively. If the maximum flow stress obtained in constant-crosshead-speed tests (see Table III) is taken as σ, the Arrhenius plot approach reported by Pilling and Ridley [1] can be used to determine the activation energy. This approach is based on the assumption that the strain rate depends on temperature at a given stress rather than the reverse (i.e., that flow stress is a function of temperature at a given strain rate). For this assumption to be valid, the flow stress must lie within the superplastic deformation region. In our example, which is based on data obtained for Weldalite™ 049 over the temperature range 820 to 940°F, we selected stresses of 1600, 2200, and 2800 psi. If it is

assumed that the strain-rate sensitivity at each temperature exhibits very little variation, then the term $(1/m)\ln(\sigma)$ can be taken as constant. The strain rates corresponding to selected temperatures can then be read from maximum flow stress vs strain rate curves (Fig. 6) and plotted vs 1/T (Fig. 7). Since the slope of this Arrhenius plot is equivalent to -Q/R, the activation energy for superplastic flow can be easily calculated. For Weldalite™ 049, the calculated values for Q are 133, 130, and 151 kJ/mol at stresses of 1600, 2200, and 2800 psi, respectively.

Alternatively, the activation energy for superplastic flow can simply be evaluated by plotting the maximum flow stress obtained in constant-crosshead-speed tests against 1/T at various initial strain rates (Fig. 8). The slopes of the curves are equivalent to mQ/R. If we assume that the strain-rate sensitivity, m, at each initial strain rate exhibits little variation, and use the m value shown in Fig. 5, then we obtain activation energies for superplastic flow of 113, 130, 142, 161, and 217 kJ/mol for initial strain rates of 6×10^{-4}, 1×10^{-3}, 2×10^{-3}, 4×10^{-3}, and 8×10^{-3} s^{-1}, respectively. It must be pointed out that the aforementioned assumptions used can introduce variation into these activation energy calculations.

3.0 EVALUATION OF MICROSTRUCTURE

To evaluate the microstructures of SPF tensile specimens with different thermal or mechanical histories three types of specimens were examined metallographically: one cut from as-received material, one cut from the gauge section of a tensile specimen that

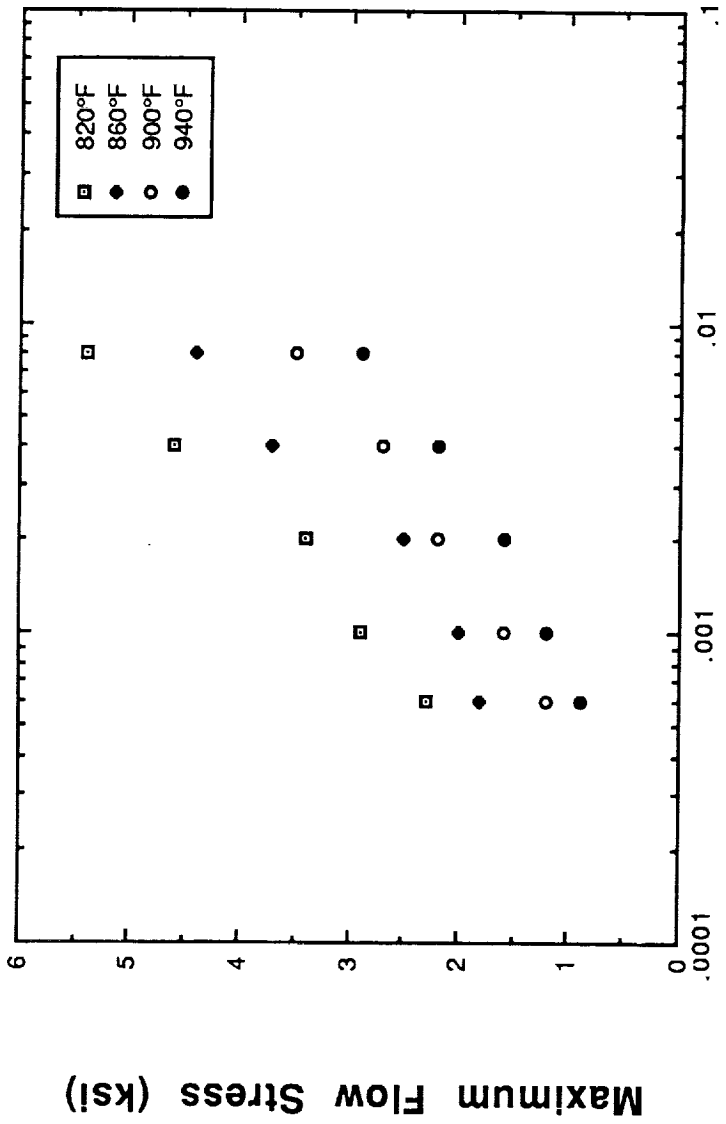

Fig. 6. Maximum flow stress vs strain-rate at various deformation temperatures for Weldalite™ 049.

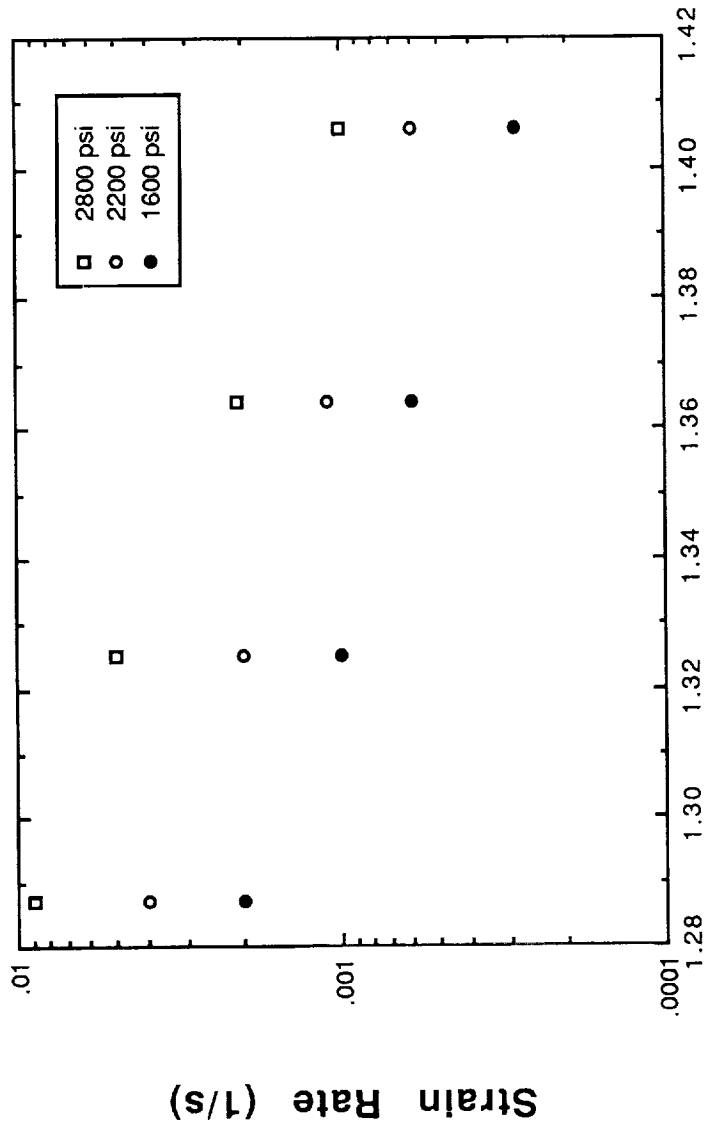

Fig. 7. Strain rate vs 1/T (absolute temperature, K) for Weldalite™ 049.

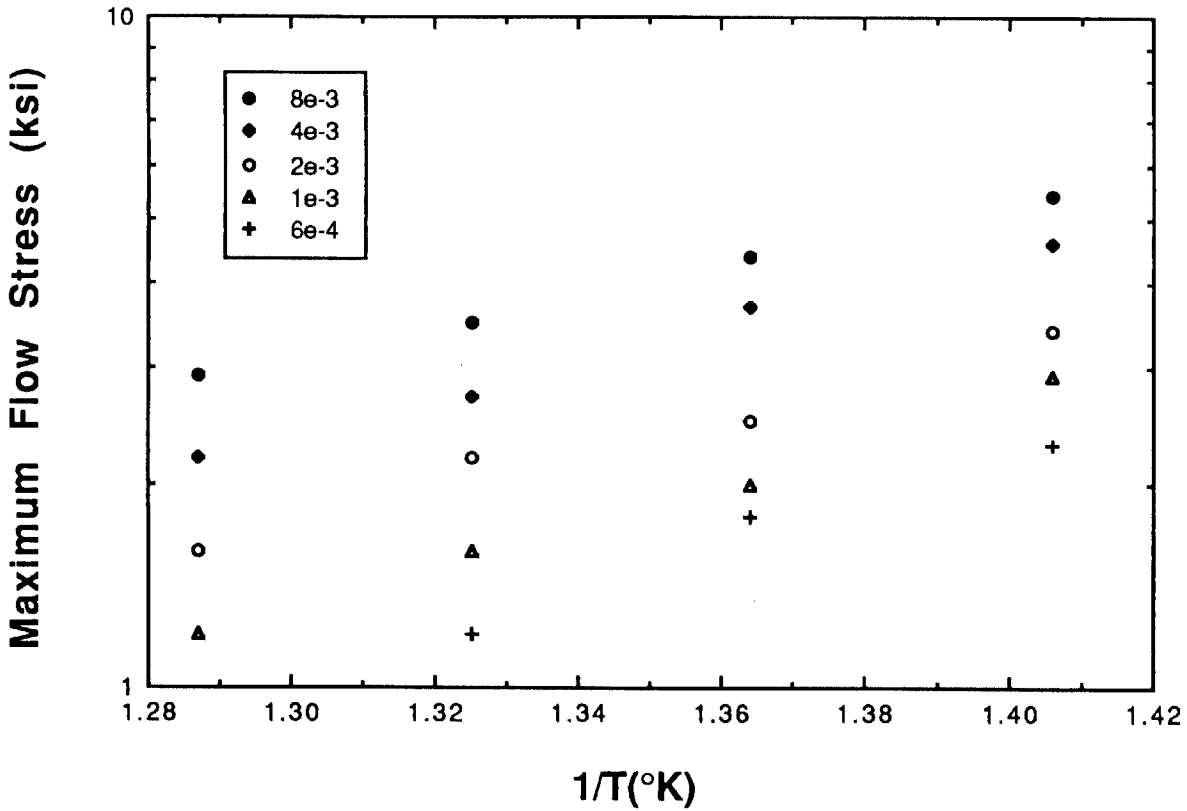

Fig. 8. Maximum flow stress vs 1/T (absolute temperature, K) at various strain rates for Weldalite™ 049.

was uniaxially deformed at a particular temperature and strain rate, and another cut from the grip area of the same specimen as the second. Therefore, the third specimen was exposed to an elevated-temperature environment but experienced no deformation. The specimens for this microstructural examination were sectioned to allow observation of the longitudinal and short transverse (L-ST) plane, then ground, polished, and anodized, and observed under polarized light.

The microstructure of the as-received material (Fig. 9) shows a typical laminar rolling structure either without or with only very slight recrystallization. That is, most grains in the as-received condition are elongated along the rolling direction. Therefore, a fine grain structure, a prerequisite for superplastic flow, is achieved by in-situ recrystallization during superplastic deformation rather than as a result of prior thermomechanical treatment.

The microstructure of the grip specimen, which was exposed to elevated temperature without experiencing deformation, indicates partial recrystallization (Fig. 10). The recrystallization at 940°F is more extensive than that at 820°F. Because the material in the grip was not subjected to deformation, the recrystallization is clearly static recrystallization [2], that is, it proceeds in the absence of deformation. Comparison of the microstructures at different elevated temperatures shown in Fig. 10 indicates that the extent of the static recrystallization depends on exposure temperature: the higher the temperature, the greater the recrystallization rate, as expected.

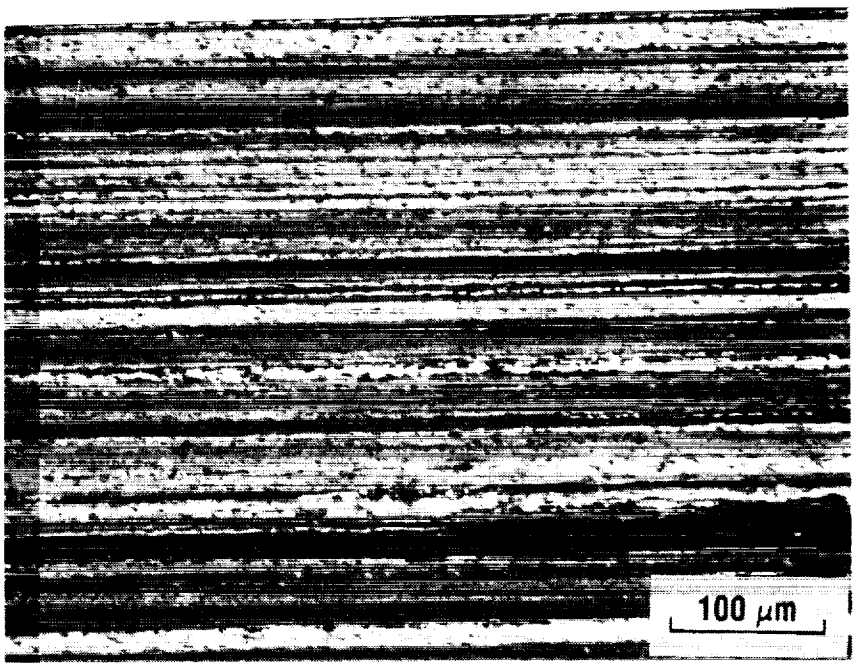

Fig. 9. Microstructure of Weldalite™ 049, processed to induce superplasticity, in as-received condition.

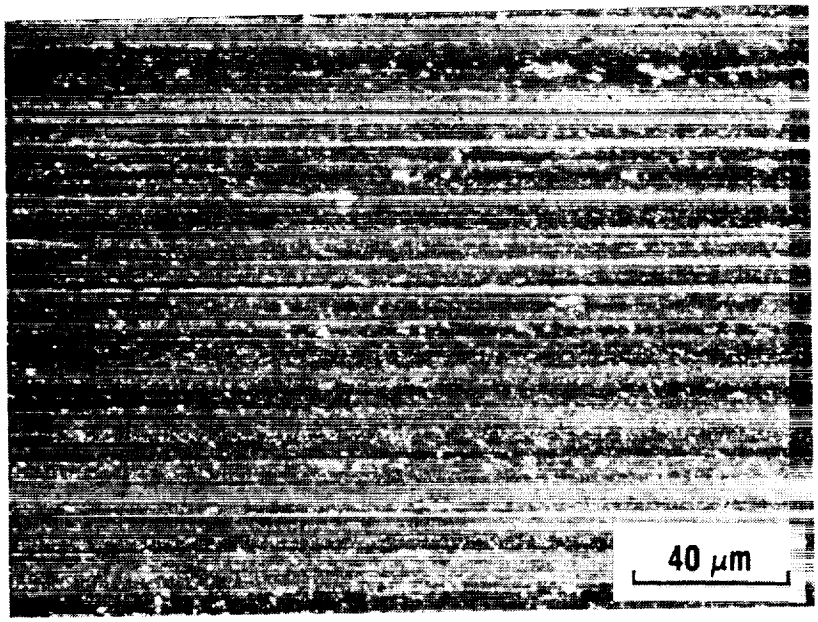

(a) 820°F

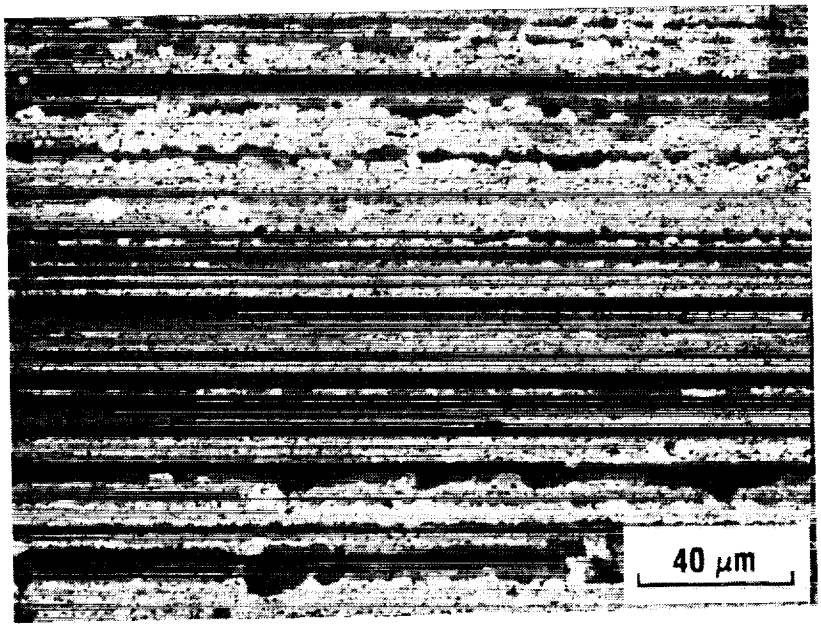

(b) 940°F

Fig. 10. Microstructure of Weldalite™ 049 at grip sections exposed to elevated temperatures.

The series of photos in Fig. 11 represents the sequence of microstructural change in a specimen tested at 940°F and an initial strain rate of $6x10^{-4}$ s^{-1}. These photos were taken from the transition area between the grip and the gage section, where specimen thickness decreased gradually from 0.125 inch (equivalent to a zero thickness strain) to 0.030 inch (equivalent to a thickness strain of 317%). Therefore, the materials experienced the same thermal history but different deformation. As seen in Fig. 11a (same as Fig. 10b), the alloy exhibits a certain amount of static recrystallization and, on heating to the superplastic temperature, develops small sub-grains at the grip where there was no deformation during the tensile test. Subsequently, the subgrain structure changes during deformation and the typical boundary misorientation angle increases with strain (Figs. 11 b, c, d, and e). The recrystallization is fully complete at the gage section with a uniaxial strain of about 671% (Fig. 11f), where no more laminar rolling structure can be seen and the as-received elongated grains are completely replaced by equiaxed grains.

This microstructural change with increasing superplastic deformation suggests that Weldalite™ 049 that is processed by Reynolds' proprietary thermomechanical technique exhibits "deformation-induced" recrystallization during superplastic deformation. It has been found that Al-based alloys may undergo superplastic deformation in either of two conditions: (1) a fully recrystallized condition where there usually exist fine equiaxed grains; and (2) a cold-worked or warm-worked condition, where there exists a highly deformed, as-rolled structure, i.e., a laminar

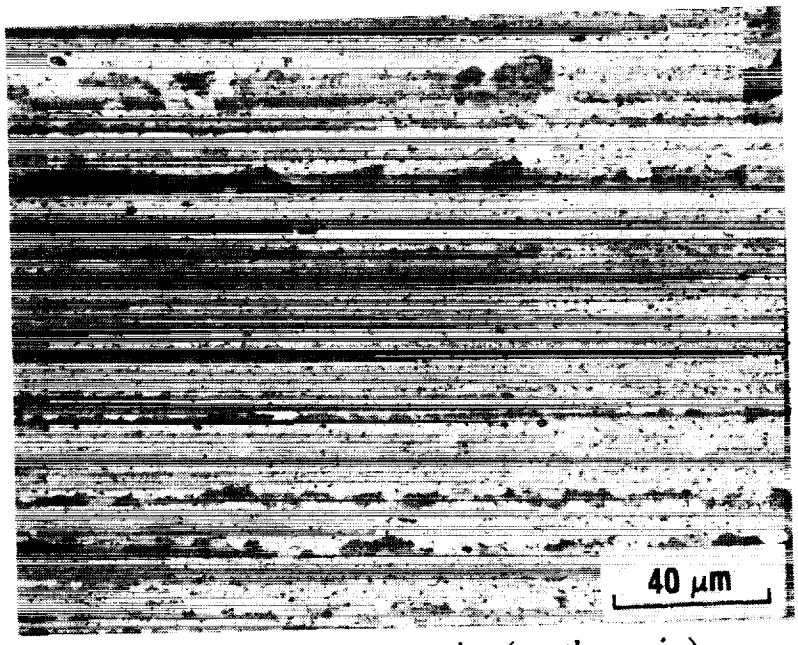

(a) 0% thickness strain (at the grip)

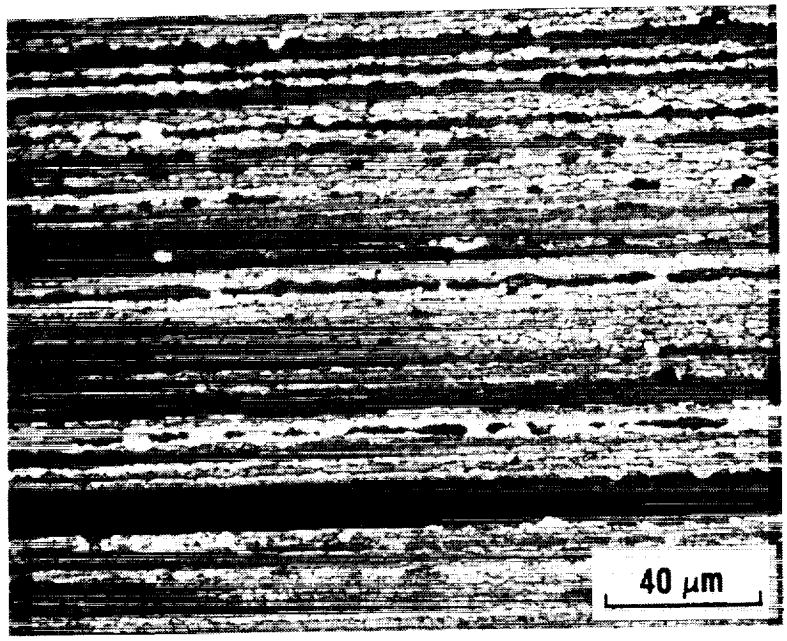

(b) 10% thickness strain

Fig. 11 Deformation-induced recrystallization at the transition area between the grip and the gage section of a specimen tested at 940°F and an initial strain rate of 6×10^{-4} s^{-1}. (superplastic elongation of 671%.)

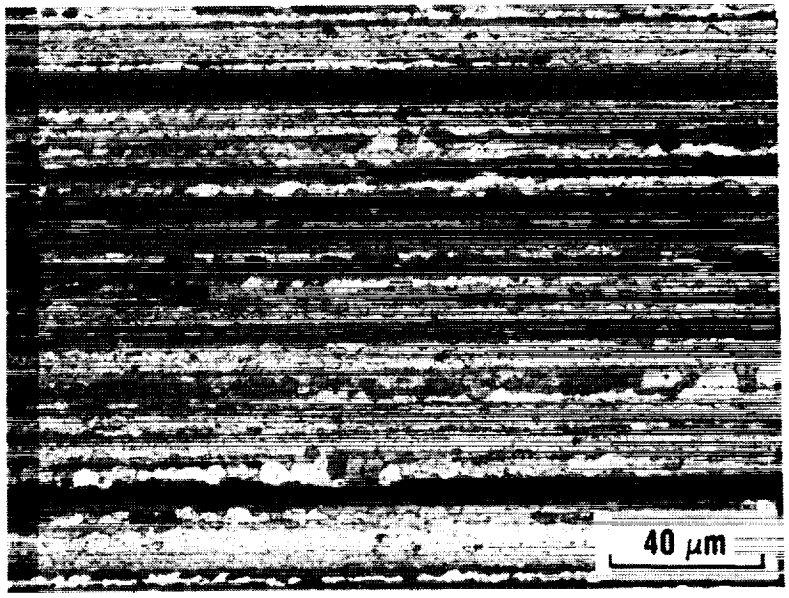

(c) 32% thickness strain

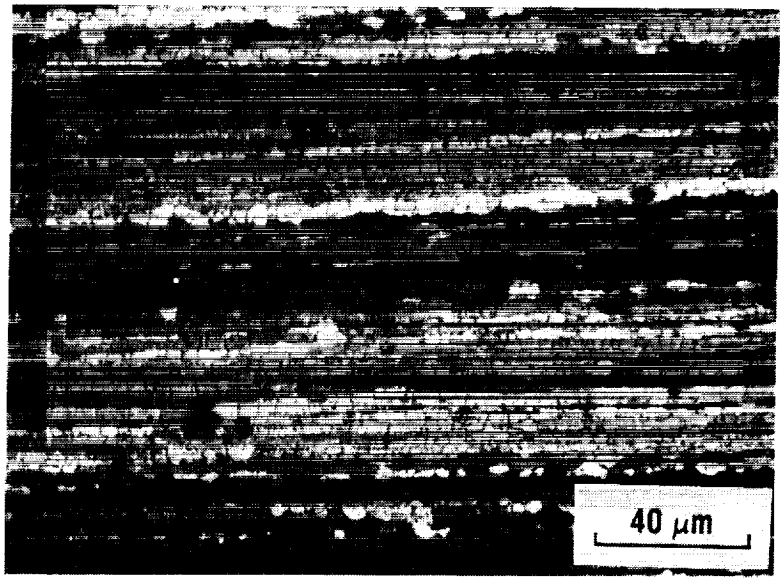

(d) 50% thickness strain

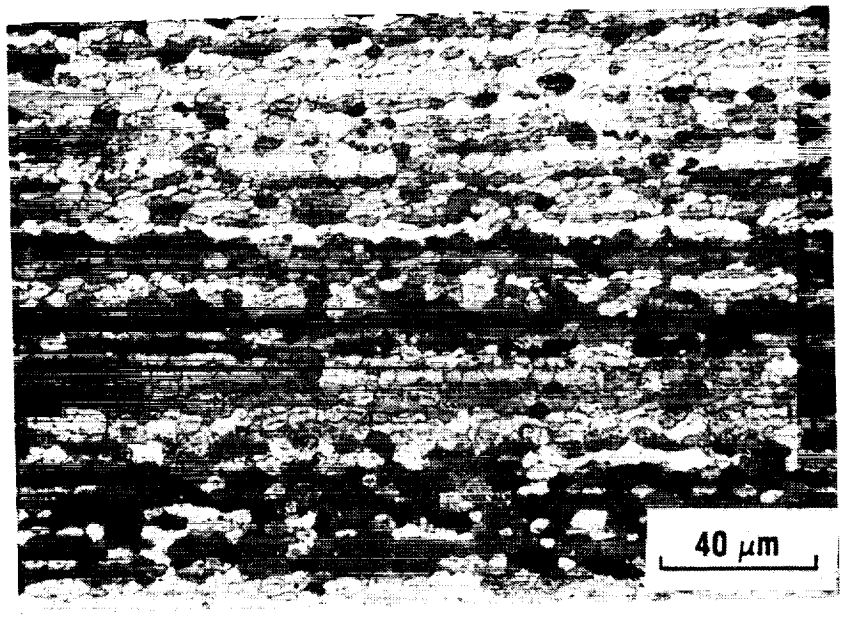

(e) 94% thickness strain

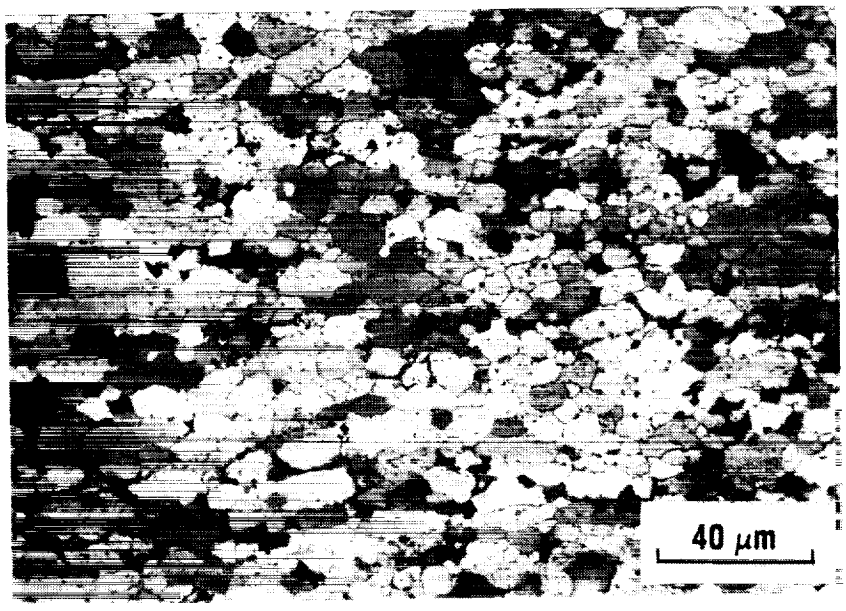

(f) 317% thickness strain (at the gage section)

structure with elongated grains along the rolling direction. It is obvious that Weldalite™ 049 most likely fits the second case, i.e., alloys which undergo recrystallization during superplastic deformation by a continuous reaction which has been termed deformation-induced recrystallization or continuous dynamic recrystallization [3].

The deformation-induced recrystallization in Weldalite™ 049 alloy is strongly dependent on the deformation temperature. Figure 12 shows the sequence of microstructural changes with increasing deformation for a specimen at the same initial strain rate as in Fig. 11 but at a much lower temperature: 820°F instead of 940°F. The comparison between Fig. 11 and Fig. 12 indicates that the deformation-induced recrystallization rate at the higher temperature is greater.

Figures 11 and 12 also show that the alloy exhibits considerable dynamic grain growth at all test temperatures, i.e., the grain size increases with increasing deformation. At the lower test temperature (820°F), the grains in the grip as well as in the gage section are smaller than those at 940°F: about 2 vs 5 microns in the grips, and 10 vs 25 microns in the gage sections.

3.1 Cavitation and Failure Mechanism

In aluminum alloys, cavitation often occurs during superplastic deformation, particularly without applied back pressure. In general, cavities nucleate at the grain boundaries and their subsequent growth and coalescence leads to premature failure. Weldalite™ 049

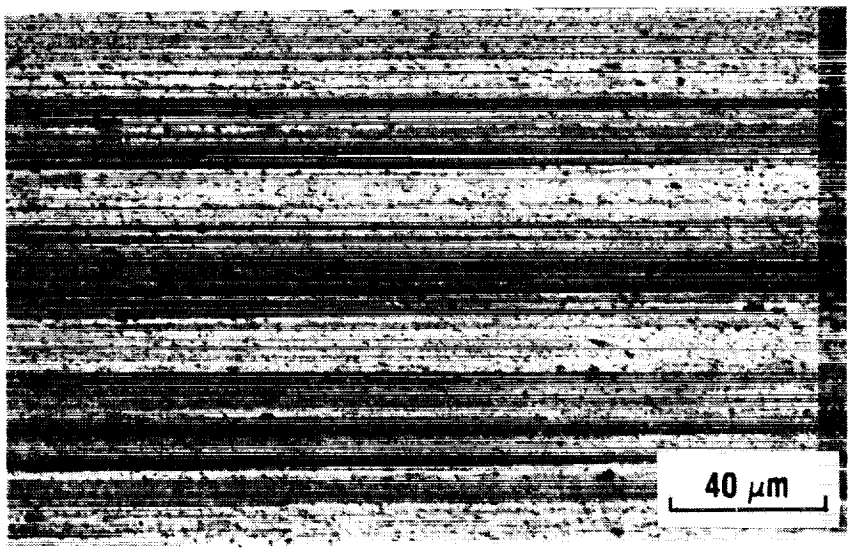

(a) 0% thickness strain (at the grip)

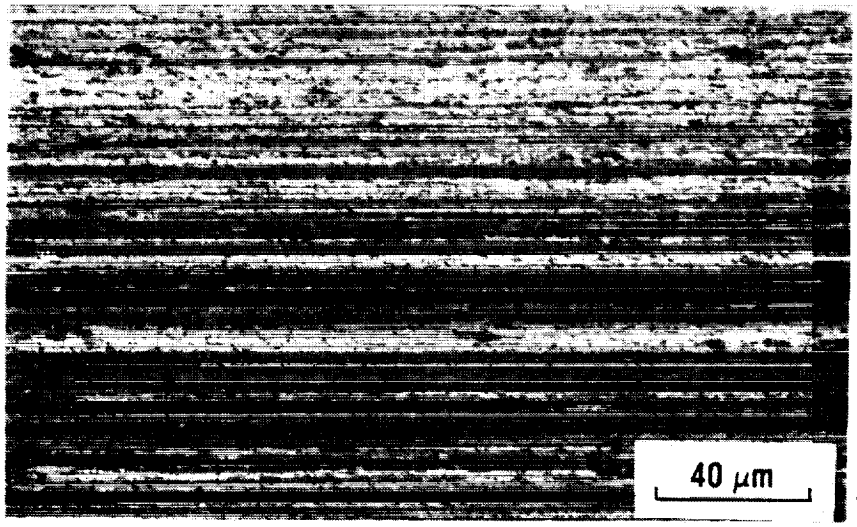

(b) 10% thickness strain

Fig. 12. Deformation-induced recrystallization at the transition area between the grip and the gage section of a specimen tested at 820°F and an initial strain rate of 6×10^{-4} s^{-1} (superplastic elongation of 560%).

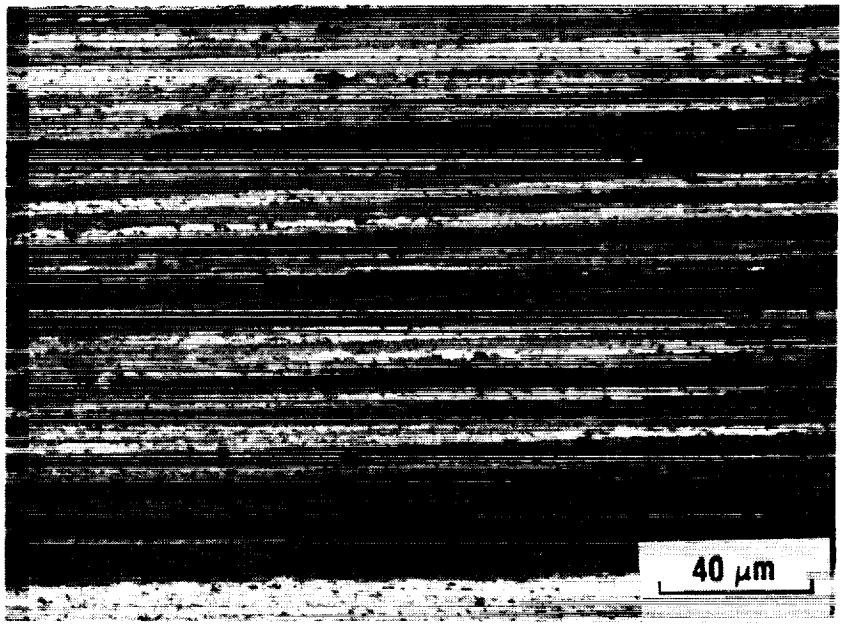

(c) 43% thickness strain

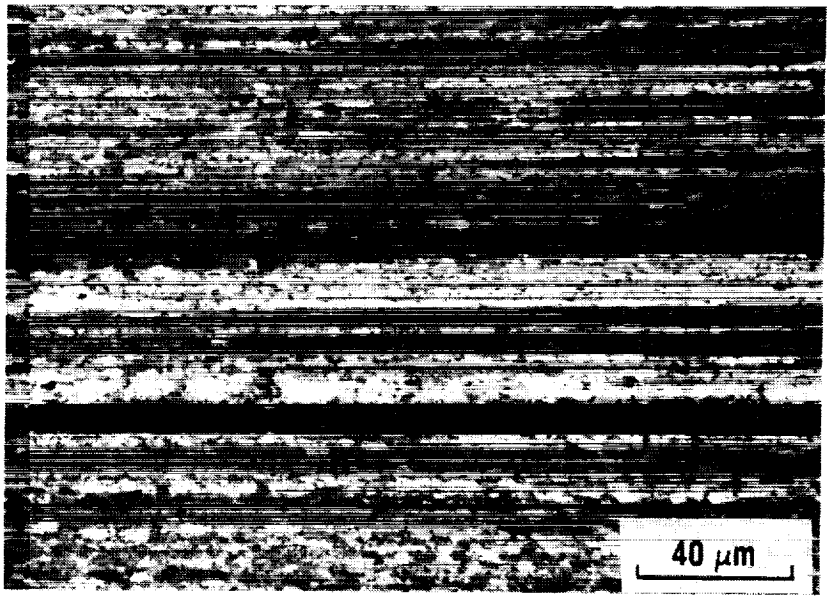

(d) 100% thickness strain

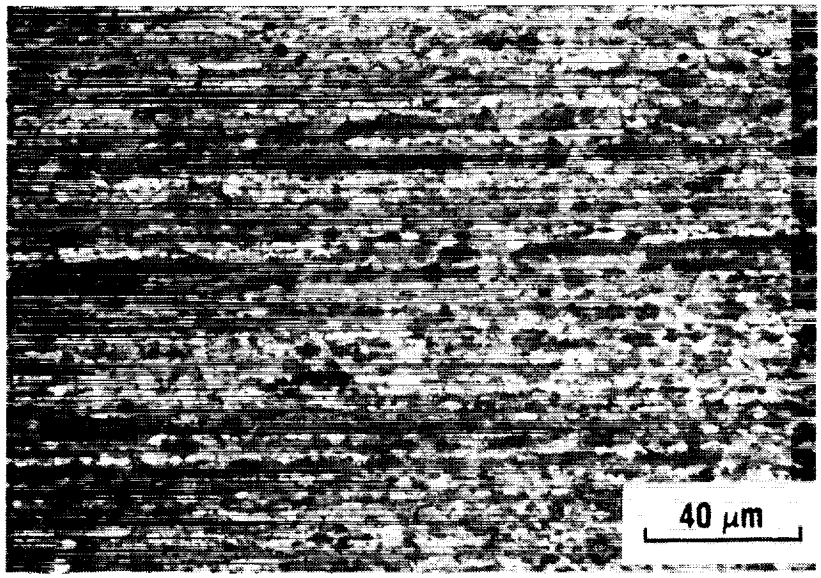

(e) 175% thickness strain

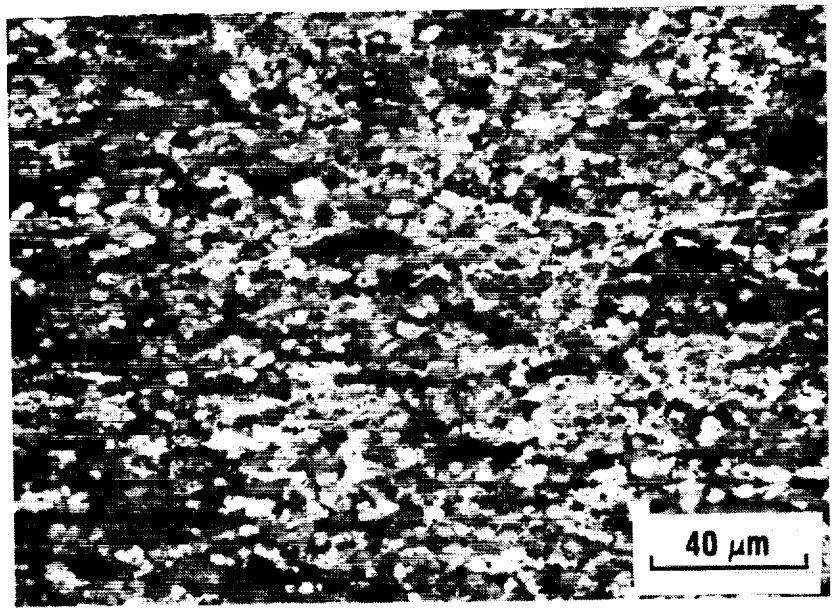

(f) 535% thickness strain (at the gage section)

tested at elevated temperatures without back pressure attains high strains, but also develops severe cavitation (Fig. 13). Because the growth of cavities is a thermally activated process, cavitation is much more severe at 940°F than at 820°F. In all of our uniaxial tensile tests to assess SPF, fracture occurred as the result of interlinking of internal cavities. Figure 14 shows a typical pseudo-brittle fracture of Weldalite™ 049 caused by cavitation.

4.0 BIAXIAL SUPERPLASTIC FORMABILITY STUDY

To evaluate biaxial superplastic formability of the alloy, we fabricated two kinds of hardware components from Weldalite™ 049 using superplastic forming technology: semispherical domes and rectangular pans (or "loaf-pans").

4.1. Semispherical Domes

The semispherical domes were fabricated at the Rockwell International Science Center, Thousands Oaks, CA. Four 5- x 5-in. long by 0.125-in.-thick sheet panels were cleaned with a wire brush, and circular grid (0.1-in.-diameter) patterns were printed onto both sides of each panel. Semispherical domes with a diameter of 2.5 in. (Fig. 15) were fabricated at different forming temperatures and strain rates with and without back pressure. The domes were deformed to failure to identify the SPF limits. Testing parameters and results are shown in Table V. The initial forming pressure for the dome was determined based on the following equation reported by Z. X. Guo, J. P. Pilling, and N. Ridley [4]:

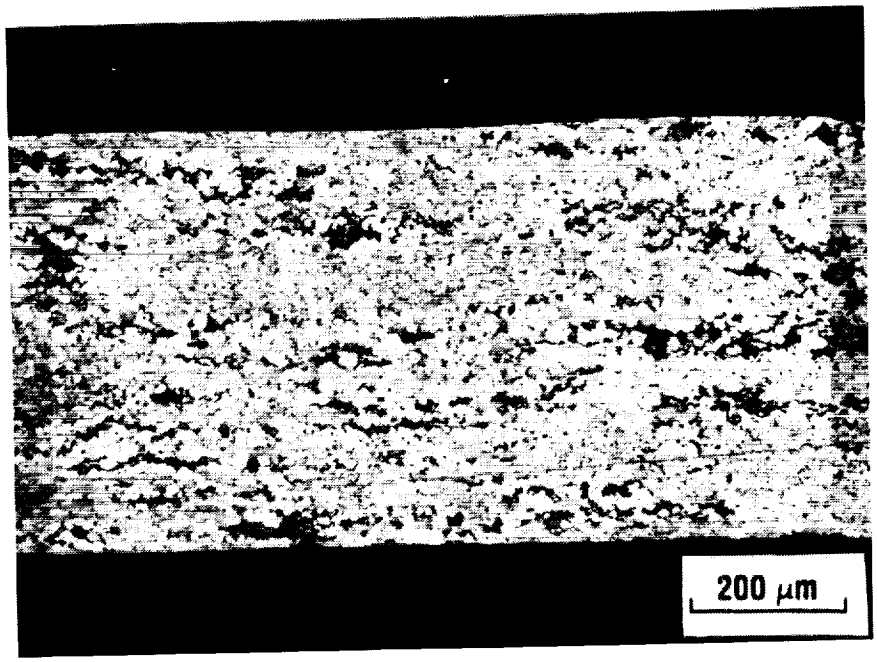

(a) 820°F

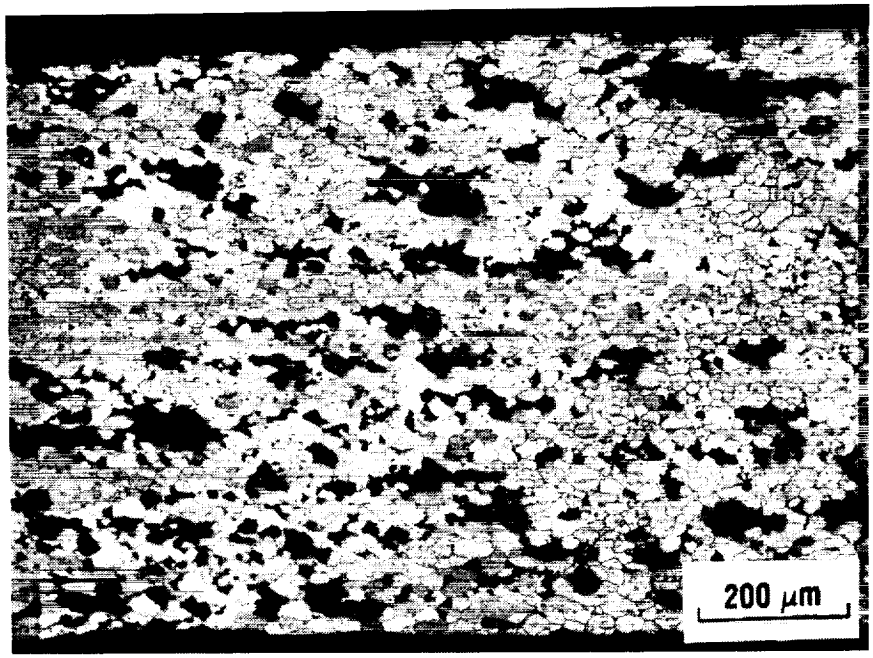

(b) 940°F

Fig. 13. Initiation and growth of cavities during superplastic deformation at an initial strain rate of 6×10^{-4} s^{-1}.

Fig. 14. A shadowgraph of the fractured specimen of Weldalite™ 049, tested in superplastic deformation at 900°F without back pressure. A flat pseudo-brittle fracture is noted.

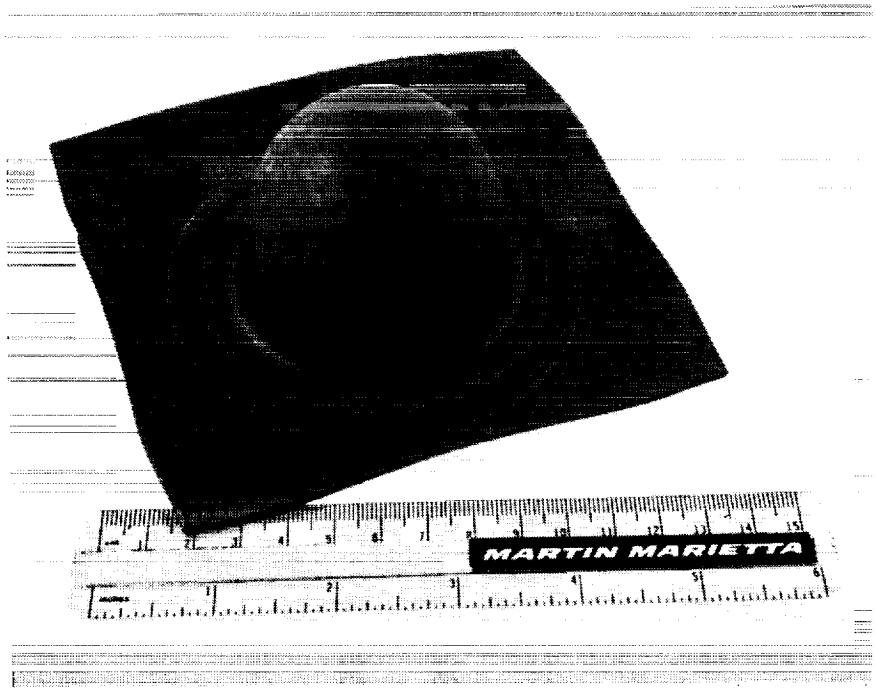

Fig. 15. Superplastically formed semispherical dome.

TABLE V

SPF Forming Parameters for Semispherical Domes of Weldalite™ 049

Dome Number	Temperature (°F)	Init. Forming Pressure (psi)	Back Pressure (psi)	Deformation Time (min)	Thickness Strain (%)	Mean Strain Rate (s^{-1})
1	940	255	0	6	287	8.0×10^{-3}
2	900	255	0	6	319	8.9×10^{-3}
3	900	185	0	8	369	7.7×10^{-3}
4	900	150	0	40	555	2.3×10^{-3}
5	860	150	400	40	458	1.9×10^{-3}
6	860	100	400	40	660	2.8×10^{-3}
7	860	150	600	38	1020	4.5×10^{-3}

$$\sigma = \frac{Pr}{8t}\left(H + \frac{1}{H}\right) \qquad (6)$$

or

$$P = \frac{8\sigma t}{r\left(H + \frac{1}{H}\right)} \qquad (7)$$

where P is the forming pressure; σ is the flow stress; and t, r, and H are the dome apex thickness, the radius of the die, and the relative dome height (the ratio of dome height and die radius), respectively. Based on the assumption of constant relative dome height, equation (7) can be simplified to

$$P = K\ \sigma\ t / r \qquad (8)$$

where K is a constant. Because the K value is determined by the dome's geometrical configuration and is affected by the definition of the flow stress, K could vary between 1 and 4. In our work, K was obtained experimentally.

The data obtained from the SPF tensile tests are necessary for accurately estimating the forming pressure required to make a SPF part, and thereby increasing the probability of successful fabrication. However, it is difficult to define a meaningful flow stress value from the load-displacement curves. The true stress vs elongation curves generated from the load-displacement curves obtained at constant crosshead speed (Fig. 2) indicate that the flow stress in hot tensile tests has no steady state value. Therefore, the maximum stress shown in Fig. 2 was chosen as the flow stress for calculation of the forming pressure. For example, the maximum flow stress for the specimen tested at 940°F and 4 x 10^{-3} s^{-1} was 2.2 ksi, the thickness of the as-

received sheet was 0.125 inch and the radius of the die was 1.25 inch; therefore, the forming pressure would be about 220 psi assuming K=1. Because the apex thickness decreases during superplastic forming, the forming pressure must be reduced accordingly. The gas pressure profile for forming dome #4 is shown in Fig. 16.

Since there is no way to detect the in-situ thickness and the position of the dome apex, the ratio of the apex thickness strain at fracture to the time needed to reach fracture is used to estimate the mean strain rate. On this basis the best apex thickness strain was found to be more than 1000% at the SPF forming temperature of 860°F and the mean strain rate of 4.5×10^{-4} s^{-1} with a back pressure of 600 psi.

The strain and thickness variation along the meridian of each dome is estimated by measuring the variation of the diameter of the circular grid. If we assume that the volume of each circular grid disc is constant during SPF forming, then

$$V_i = V_f \tag{9}$$

or

$$A_i t_i = A_f t_f \tag{10}$$

or

$$\frac{1}{4}\pi d_i^2 t_i = \frac{1}{4}\pi d_f^2 t_f \tag{11}$$

where V, A, and d represent volume, circular area, and diameter of the circular grid disc, respectively, and the subscripts i and f represent the initial and final states, respectively. This equation can be written as follows:

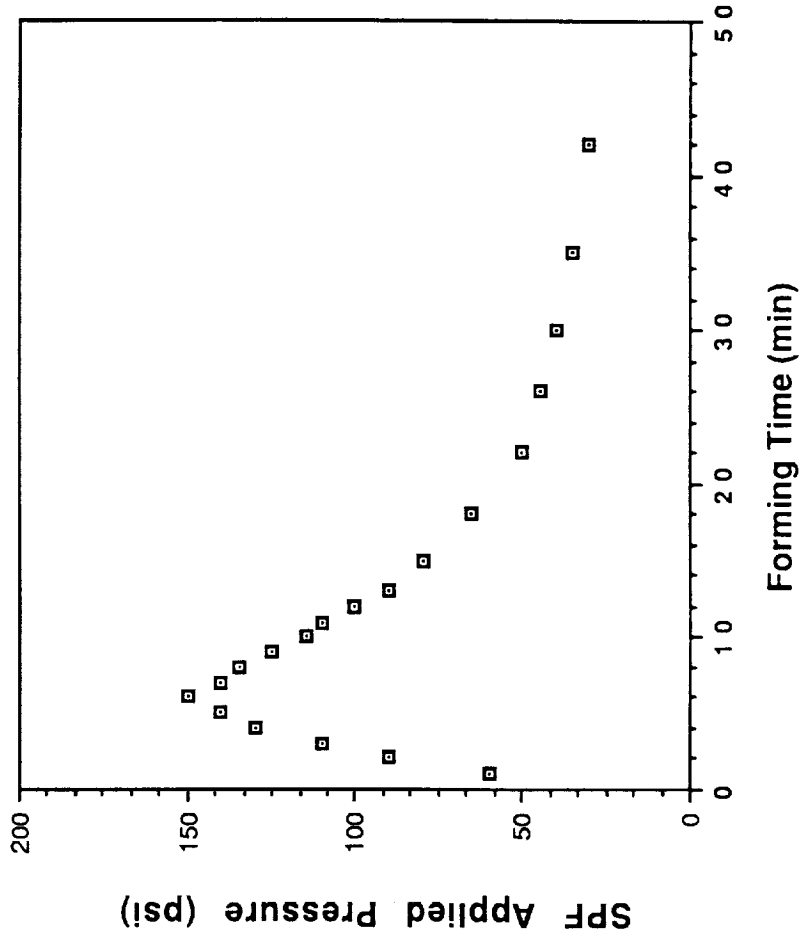

Fig.16. Gas pressure profile for superplastically formed semispherical dome #4.

$$\frac{d_f^2}{d_i^2} = \frac{t_i}{t_f} \qquad (12)$$

Therefore, the thickness strain (ε_{thick}) can be obtained from:

$$\varepsilon_{thick} = \frac{t_i - t_f}{t_f} = \frac{d_f^2 - d_i^2}{d_i^2} \qquad (13)$$

The variation of thickness strain along the meridian of the dome is shown in Fig. 17 as a function of the normalized position, which is defined as the ratio of the original position of each circular grid before superplastic forming and the dome radius. Therefore, the normalized positions 0 and 1 represent the dome edge and dome apex, respectively.

4.2. Rectangular Pans

Rectangular pans were fabricated at NASA Langley Research Center, Hampton, VA. Each loaf-shaped pan with a dimension of approximately 8 x 2.5 x 3 inches (Fig. 18) were superplastically formed from an 11 x 15-inch 0.125-inch-thick sheet. Each was formed at 925°F and an estimated strain rate of 2×10^{-4} s^{-1}, with and without back pressure and post-forming pressure. Gas pressure profiles used in fabricating the pans are shown in Figs. 19-22. The gas pressurization parameters for forming the pans were selected

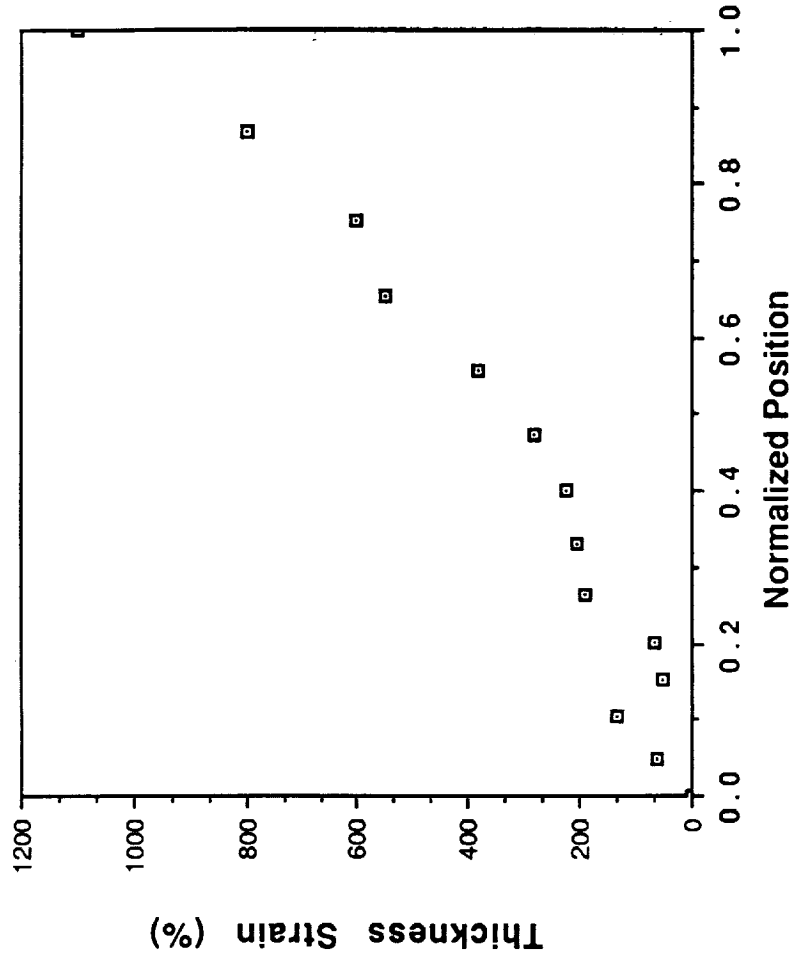

Fig. 17. Thickness strain vs normalized position along the dome meridian (normalized positions 0 and 1 represent the dome edge and dome apex, respectively).

ORIGINAL PAGE
BLACK AND WHITE PHOTOGRAPH

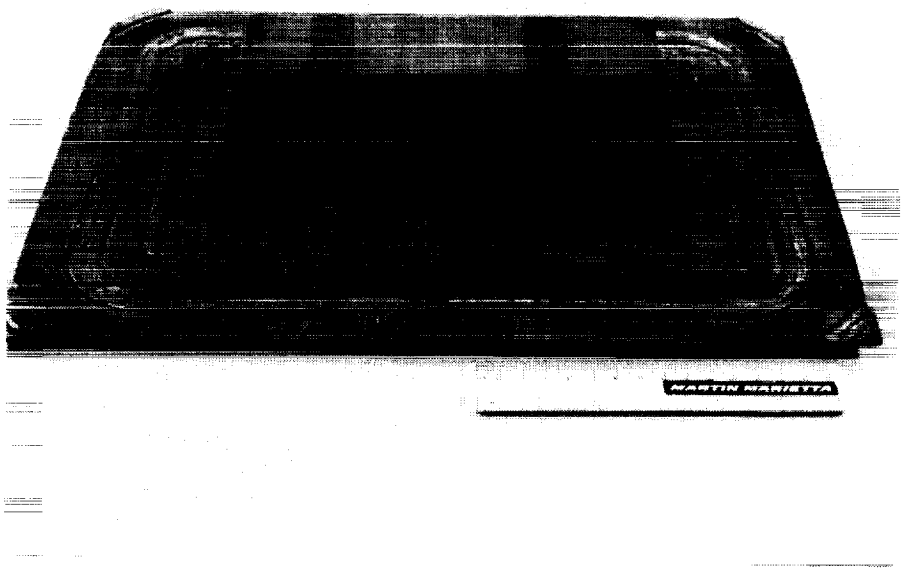

Fig. 18. Superplastically formed rectangular pan.

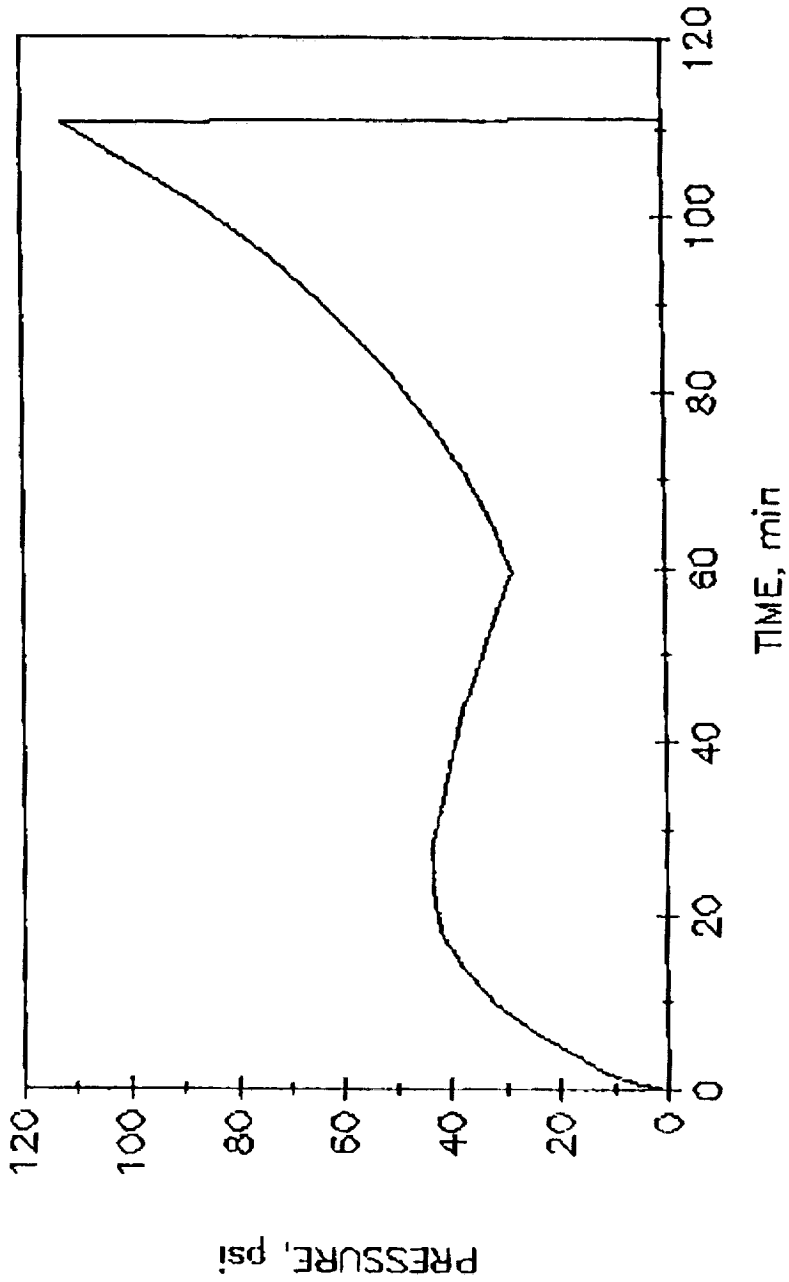

Fig. 19. Gas pressure profile for superplastically formed pan #1.

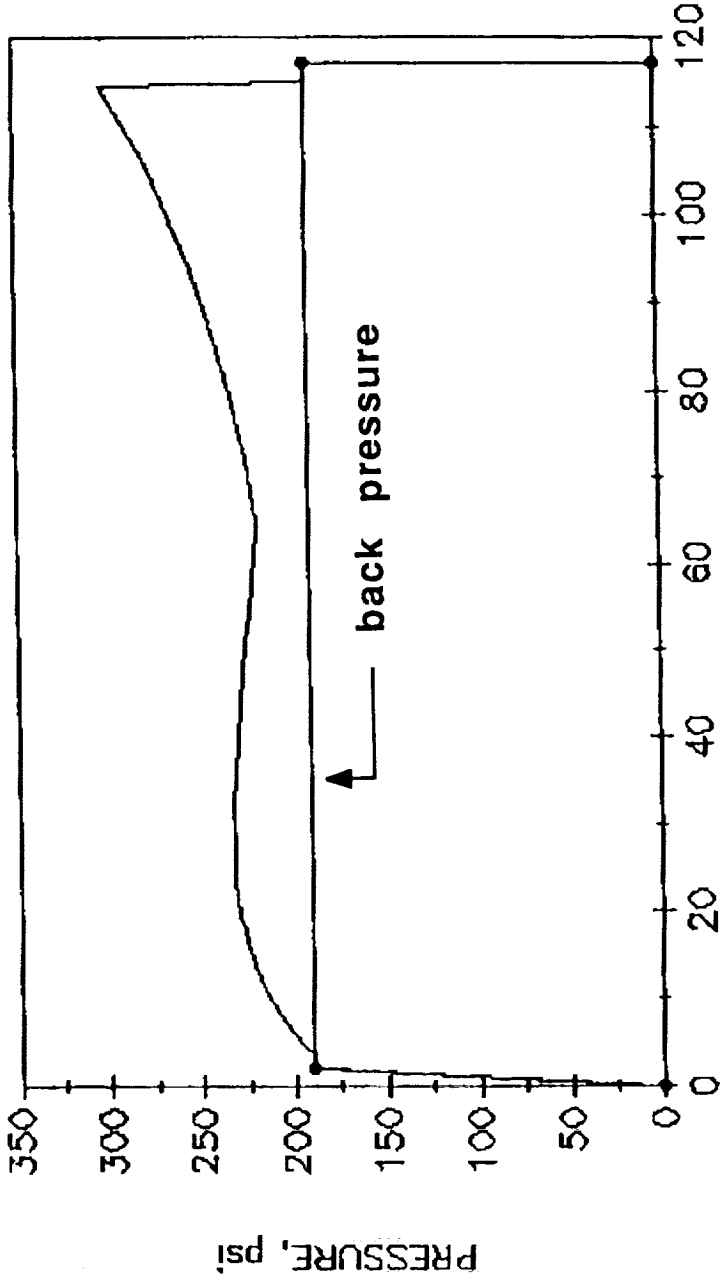

Fig. 20. Gas pressure profile for superplastically formed pan #2.

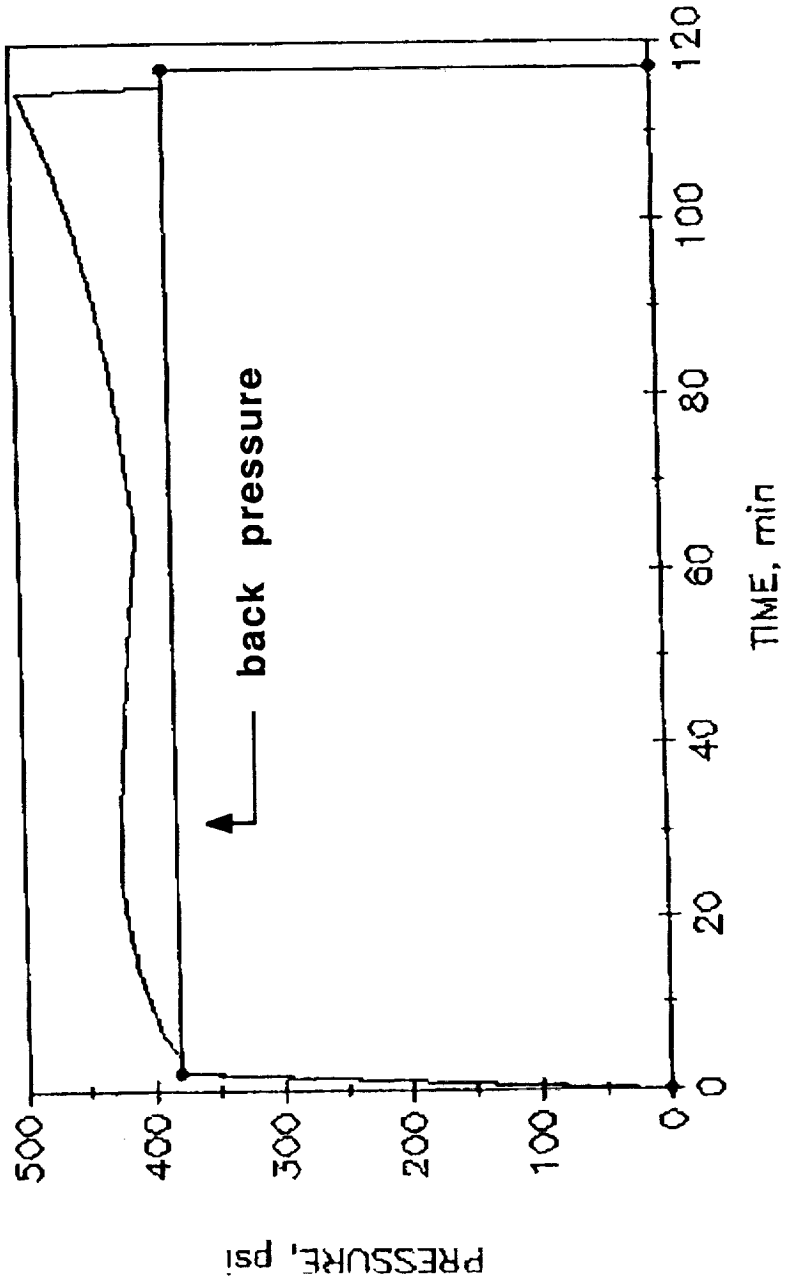

Fig. 21. Gas pressure profile for superplastically formed pan #3.

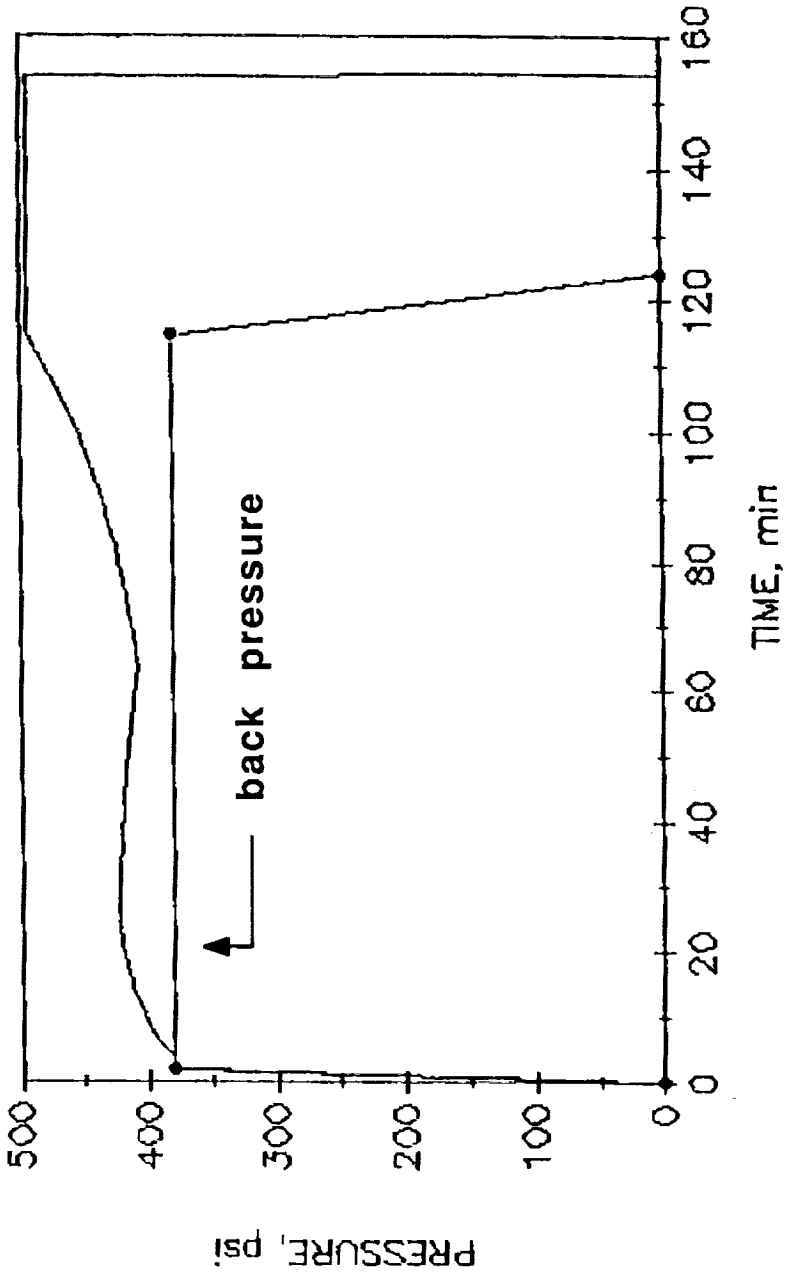

Fig. 22. Gas pressure profile for superplastically formed pans #4 and #5.

based on uniaxial tensile data on Weldalite™ 049 obtained at NASA Langley Research Center and summarized in Table VI.

Back and post-forming pressure were applied to determine the effects of a superimposed hydrostatic stress during SPF (i.e., back pressure) and a hydrostatic stress treatment following SPF (i.e., post-forming pressure) on cavitation and subsequent post-SPF behavior. Previous investigation at NASA Langley Research Center has shown that the addition of post-forming pressure collapses cavities by creep and heals them by diffusion bonding [5]. Thus, we applied an additional post-forming segment (see Fig. 22), consisting of a pressure of 492 psi for 30 minutes at the same temperature as that applied during forming. Basically, the gas pressure profiles for all pans were the same, if the effects of the back pressure and the post-forming pressure are removed from the profiles. For details of how the gas pressure profiles were selected, refer to Ref. [5].

The five rectangular pans made from Weldalite™ 049 were fabricated with no failures. The distribution of SPF deformation was studied on a transverse section cut from one of the pans. The cross section of the pan is shown in Fig. 23 and the distribution of thickness and thickness strain are shown in Figs. 24 and 25, respectively. Here, the engineering thickness strain is defined as in Eq. (13):

$$\varepsilon_{thick} = \frac{t_i - t_f}{t_f}$$

where t_i and t_f represent the initial and final thickness strain, respectively. The maximum thickness strain of 228% was observed at

TABLE VI

SPF Forming Parameters for Rectangular Loaf-Pans* of Weldalite™ 049

Pan Number	SPF Forming Temperature (°F)	Planned Strain Rate (s^{-1})	Back Pressure (psi)	Post-Forming Pressure (psi)
#1	925	$2x10^{-4}$	0	0
#2	925	$2x10^{-4}$	190	0
#3	925	$2x10^{-4}$	380	0
#4	925	$2x10^{-4}$	380	492
#5**	925	$2x10^{-4}$	380	492

* Pans fabricated at NASA Langley Research Center.

** This pan was stuck in the die, slowly cooled overnight, and removed at 360°F.

ORIGINAL PAGE
BLACK AND WHITE PHOTOGRAPH

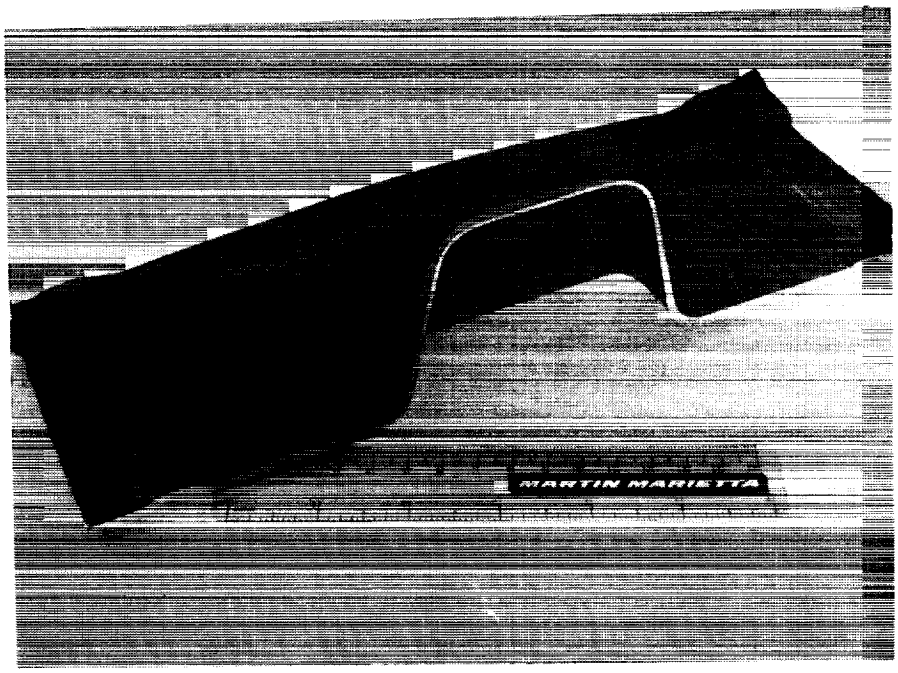

Fig. 23. Cross section of a superplastically formed rectangular pan.

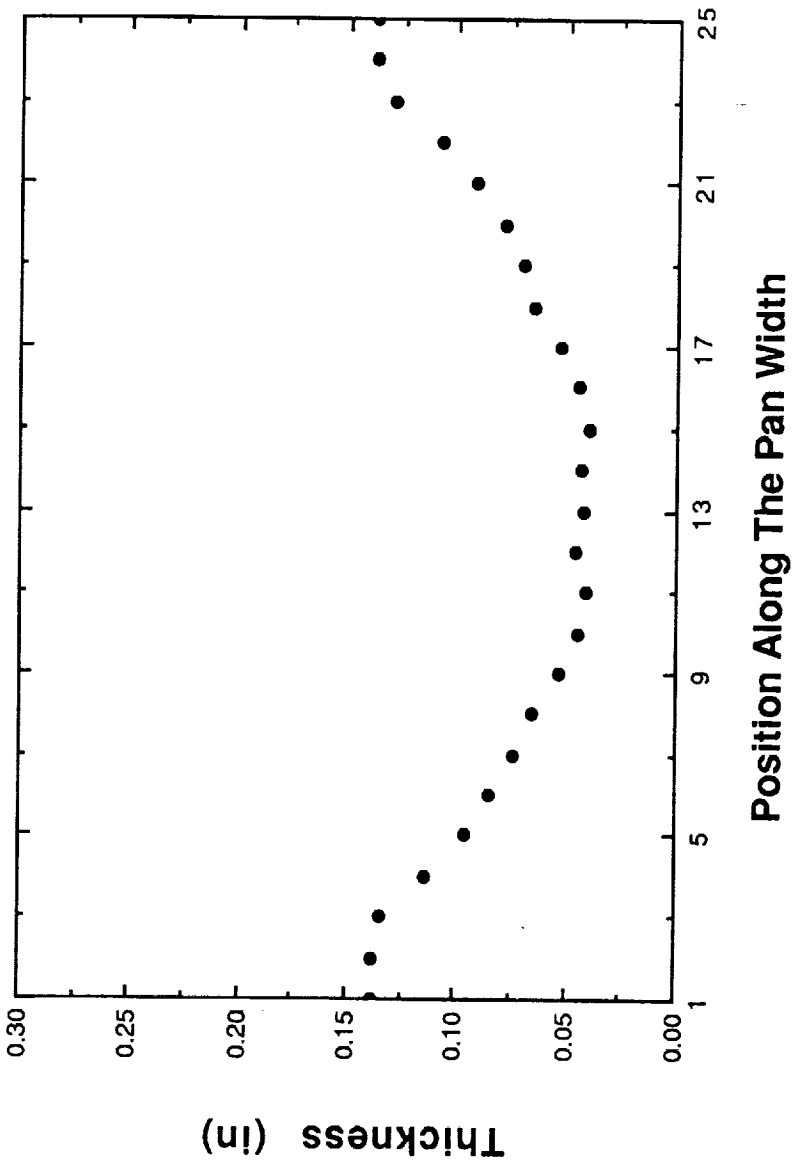

Fig. 24. Thickness vs position along a pan's meridian.

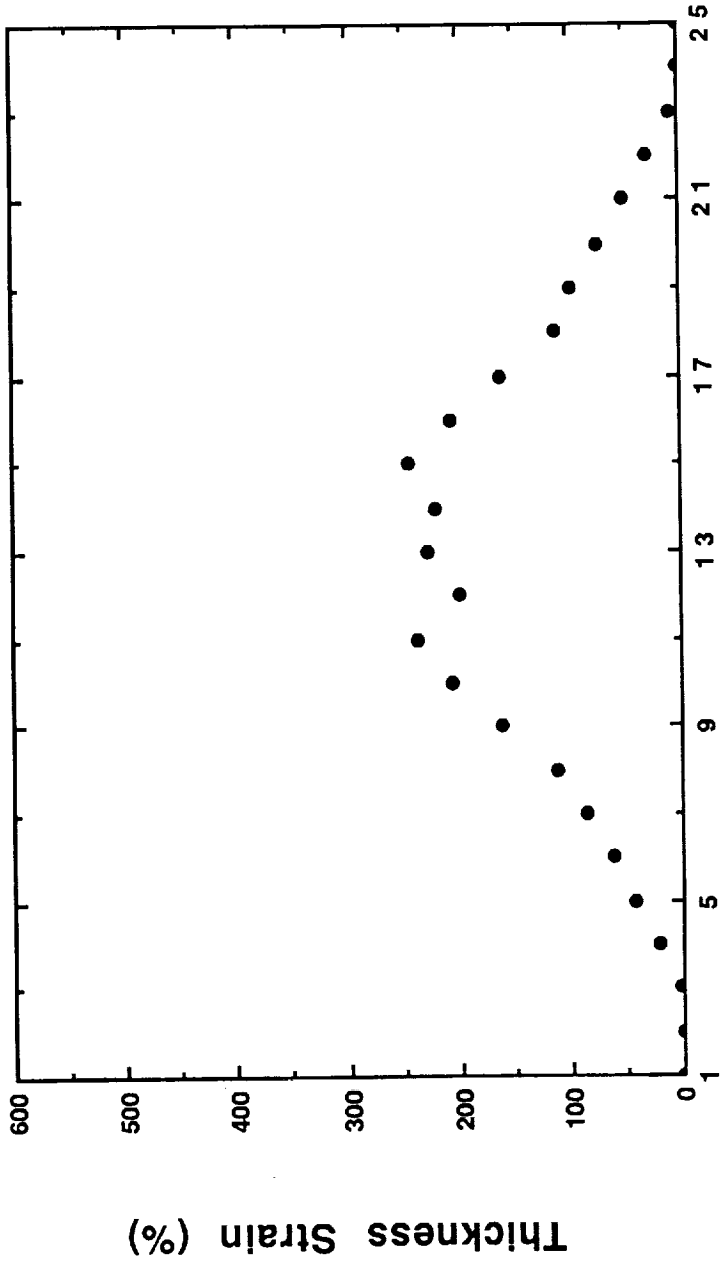

Fig. 25. Thickness strain vs position along a pan's meridian.

the pan's bottom. Thickness strain also varies along the longitudinal direction: measured thickness at the bottom varied from 0.040 inch near the sidewall to 0.068 inch at the center.

5.0 POST-SPF MECHANICAL PROPERTIES

Evaluation of post-SPF properties of Weldalite™ 049 is one of the most important and interesting areas of this work. We evaluated post SPF properties by (1) measuring hardness and tensile properties of the alloy in different temper conditions, and (2) measuring tensile properties of the alloy in one temper condition (T6) at various temperatures (cryogenic, room, and elevated temperature).

5.1. Aging Behavior

Specimen coupons for the aging study were cut from a sidewall of a rectangular pan superplastically formed at 925°F with a back pressure of 190 psi. The coupons were solution-heat-treated, i.e., heated at 940°F for 45 minutes followed by rapid quenching in water at 68°F, and either naturally aged (T4 temper) or artificially aged (T6 temper) at 320°F, 338°F, and 356°F. The aging response was monitored using Rockwell B hardness measurements. Figure 26 shows hardness vs artificial aging-time curves for 320, 338 and 356°F, as well as natural aging. It is noted that the curves for each aging temper are very similar to those for non-SPF processed (i.e., wrought) Weldalite™ 049 aging to the same temper. For example, artificial aging at 338°F also exhibits a reversion behavior that is similar to that seen for wrought Weldalite™ 049. Aging for a short period (e.g., 5 - 45

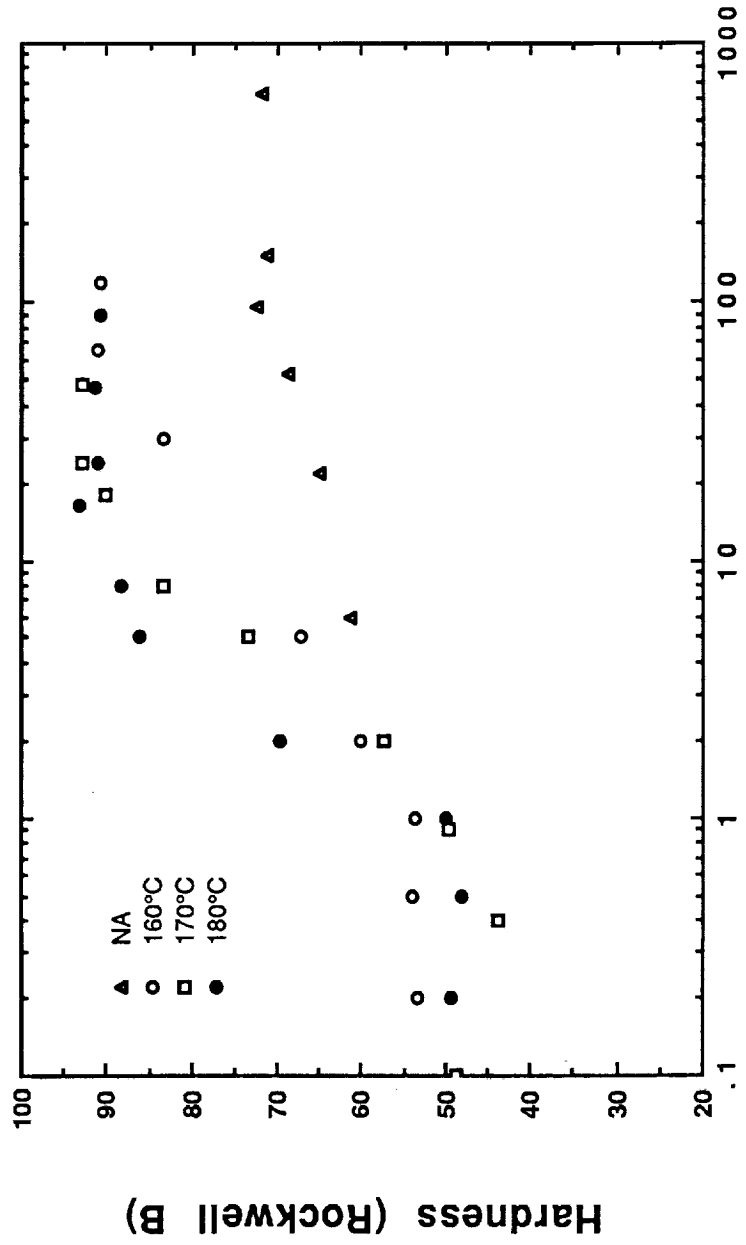

Fig. 26. Hardness vs aging-time in T4 (natural aging) and T6 (artificial aging) tempers for post-SPF Weldalite™ 049.

minutes) leads to a loss of hardness, while further aging for 20 - 24 hours results in a peak hardness of R_B 93, which is very close to the peak hardness (R_B 95) of wrought Weldalite™ 049. This reversion behavior of the post-SPF Weldalite™ 049 may be due to the same mechanism as that for the wrought alloy, i.e., to dissolution of the strengthening phases δ' and GP zones, and coarsening of the larger GP zones as observed by Gayle et al. [6] on wrought Weldalite™ 049.

5.2. Post-SPF Tensile Properties

A nonstandard subsize tensile specimen with a gage length of 0.5 inch and a width of 0.25 inch was chosen because of limited material. Tensile specimens were cut along the rolling direction from the bottom of rectangular pans, solution-heat-treated (heated at 940°F for 45 minutes followed by quenching in water), and then artificially aged to a peak hardness of about R_B 93. The thickness of the specimens varied from 0.040 to 0.065 inch (i.e., the materials experienced thickness strains between 225% and 100%), depending on their location in the pans. Eight tensile tests were performed at room temperature, two tests at elevated temperature (302°F), and three tests at cryogenic temperature (-320°F). The post-SPF aging conditions and tensile properties of these specimens as well as the SPF forming condition are summarized in Table VII. The effect of temperature on yield strength and ultimate tensile strength is shown in Fig. 27. The results of the tensile tests indicate that Weldalite™ 049 exhibits very good post-SPF mechanical properties over the temperature range considered. The room-temperature data [Table VII (a)] show yield strengths from 77.8 ksi to 84.7 ksi, ultimate strengths from 87.3 ksi to 92.2 ksi, and

TABLE VII (a)

Post-SPF Tensile Properties of Weldalite™ 049 at Room Temperature

(SPF deformation temperature = 925°F, SPF thickness strain = 100%)

Specimen Number	Back Pressure (psi)	Post-forming Pressure (psi)	Aging Condition (°F(h))	Yield Stress (ksi)	Ultimate Tensile Stress (ksi)	Elongation (%)
1-1	0	0	338(24)	77.8	87.3	7.4
3-1	380	0	338(24)	na*	92.2	7.4
4-1	380	492	338(24)	na*	90.6	6.9
1-2	0	0	356(20)	84.7	89.6	5.4
3-2	380	0	356(18)	na*	88.5	6.3
4-2	380	492	356(18)	na*	91.4	5.6

* Slippage in specimen grips precludes precise yield stress measurement. Values are likely between 80 and 90 ksi based on hardness values and comparable data for wrought Weldalite™ 049.

TABLE VII (b)

Post-SPF Tensile Properties of Weldalite™ 049 at -320°F

(SPF deformation temperature = 925°F, SPF thickness strain = 100%)

Specimen Number	Back Pressure (psi)	Post-forming Pressure (psi)	Aging Condition (°F(h))	Yield Stress (ksi)	Ultimate Tensile Stress (ksi)	Elongation (%)
1-4	0	0	338(24)	88.0	106.0	5.3
3-4	380	0	338(24)	91.5	102.8	5.8
4-4	380	492	338(24)	91.5	106.8	6.1

TABLE VII (c)

Post-SPF Tensile Properties of Weldalite™ 049 at 302°F

(0.5 h hold at temperature)

(SPF deformation temperature = 925°F, SPF thickness strain = 100%)

Specimen Number	Back Pressure (psi)	Post-forming Pressure (psi)	Aging Condition (°F(h))	Yield Stress (ksi)	Ultimate Tensile Stress (ksi)	Elongation (%)
1-5	0	0	338(24)	65.0	75.3	12.3
3-5	380	0	338(24)	61.5	70.8	8.6

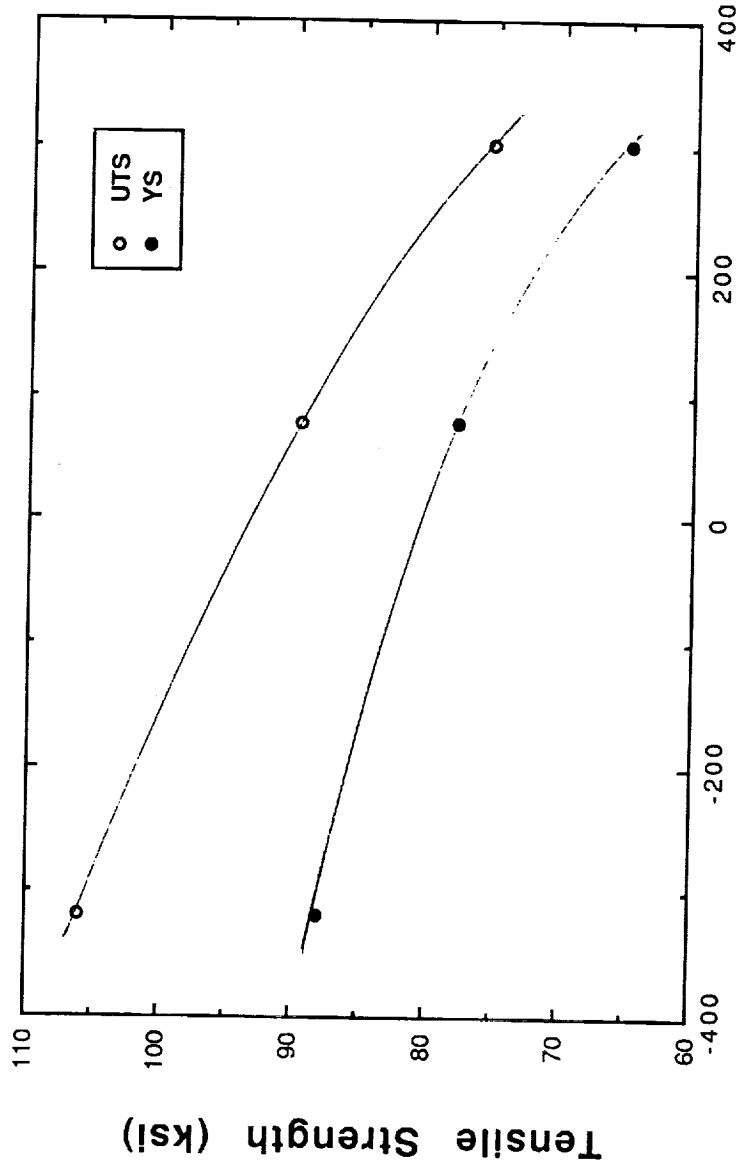

Fig. 27. Effect of temperature on post-SPF yield strength and ultimate tensile strength.

elongations from 5.4 to 7.4 percent. At -320°F, the strengths are higher (up to 91.5 ksi yield and 106.8 ksi ultimate) with elongations between 5.3 and 6.1 percent [Table VII(b)]. At +302°F with 0.5 hour exposure to the test temperature [Table VII(c)], yield strengths up to 65 ksi with ultimate strengths up to 75.3 ksi and elongations of 12.3 percent were obtained. The results shown in Table VII also suggest that back pressure and post-forming pressure in SPF-forming does not significantly affect post-SPF properties. A possible explanation is that SPF straining and SPF deformation time during the pan fabrication are not large enough or of sufficient duration to generate severe SPF cavities: thus, there is no significant loss of tensile strength due to cavitation, irrespective of the back pressure and post-forming pressure. Further microstructural examination is need to support this conjecture.

Although the post-SPF tensile strengths of Weldalite™ 049 are very high, it is not yet understood why the post-SPF strength is only 90% of that of the wrought alloy (the ultimate tensile strength of wrought Weldalite™ 049 sheet in the T6 temper can exceed 100 ksi at room temperature). The strength difference is probably due to two factors. First, the specimens for post-SPF property evaluation were significantly thinner than those used for standard tensile properties (0.06 vs 0.25 inch), which could introduce a different stress condition during tensile deformation and lead to fracture at lower stress.

Second, the materials for post-SPF property evaluation experienced a certain amount of deformation and were exposed to an elevated-temperature environment for a certain amount of time: consequently, they underwent some changes in microstructure.

Further work is needed to assess changes in grain size as well as substructure and to determine whether the distributions and relative amounts of strengthening precipitates of the alloy during or after SPF deformation are different from those of the wrought alloy.

In Table VIII post-SPF tensile properties at room temperature for Weldalite™ 049 and other major aluminum alloys in the T6 temper can be compared. The data show that Weldalite™ 049 has significantly greater post-SPF strength than other leading SPF aluminum alloys.

TABLE VIII

Comparison of Post-SPF Tensile Properties of Leading SPF Aluminum Alloys

Alloy (Composition wt%)	SPF Thickness Strain (%)	Yield Stress (ksi)	Ultimate Tensile Stress (ksi)	Elongation (%)	Ref.
Weldalite™ 049 (4.75Cu-1.3Li-0.4Mg-0.4Ag-0.14Zr)	100	85	92	7.4	
2090 (2.6Cu-2.4Li-0.2Zr)	100	46	52	NA	[7]
8090 (1.2Cu-2.5Li-0.6Mg-0.1Zr)	NA	46	61	5.5	[8]
8091 (1.8Cu-2.5Li-0.7Mg-0.12Zr)	NA	49	65	5.5	[8]
7475 (5.5Zn-2.5Mg-1.5Cu-0.2Cr)	100	72	77	NA	[9]
Supral 100 (6.0Cu-0.4Zr-0.2Mg)	75-150	44	58	10.7	[10]
Supral 220 (6.0Cu-0.4Zr-0.3Mg-0.2Si-0.1Ge)	75-150	50	59	7.1	[10]

6.0 CONCLUSIONS

1. Weldalite™ 049 exhibits very good superplasticity over a wide range of temperatures and strain rates.

(a) >900% elongation obtained in uniaxial tensile tests without back pressure.

(b) 829% elongation obtained at the solution-heat-treatment temperature (940°F) without back pressure and at a relatively high strain rate ($4x10^{-3}$ s^{-1}).

(c) >1000% thickness strain obtained in biaxial dome-forming tests with back pressure.

2. The maximum strain-rate sensitivity of a 0.5 at a deformation temperature of 900°F is observed in the strain-rate range $2x10^{-4}$ to $1x10^{-3}$ s^{-1} where high superplastic elongations (>800%) are observed.

3. The dramatic decrease seen in the true stress of Weldalite™ 049 during superplastic deformation at a constant crosshead speed is mainly caused by the decrease in the true strain rate.

4. Deformation-induced recrystallization is observed during superplastic flow.

5. Cavity coalescence is the dominant failure mechanism in Weldalite™ 049 during uniaxial superplastic deformation without applied back pressure.

6. Weldalite™ 049 displays excellent post-SPF tensile properties in the T6 temper at room, elevated, and cryogenic temperatures. At room temperature, yield strengths, ultimate strengths, and elongations up to 87.3 ksi, 92.2 ksi, and 7.4%, respectively, were obtained. The strength increased by about 10% at -320°F and decreased by about 10% at +302°F, with no significant change in elongation.

7. Weldalite™ 049 exhibited higher post-SPF tensile strengths than those reported for other leading SPF aluminum alloys.

7.0 REFERENCES

[1] L. Pilling and N. Ridley, Superplasticity in Crystalline Solids, The Institute of Metals, p. 61, 1989.

[2] J.J. Jones, H.J. McQueen, and W.A. Wong, "Deformation under Hot-Working Conditions", Iron Steel Inst., London (Special Rep. No. 108), p. 49, 1968.

[3] B. Ren and C.H. Hamilton, "The Microstructural Characteristics of an Al-Li-Cu-Mg-Zr Alloy during the Initial Stage of Superplastic Deformation", in Proceedings of an International Conference on SPF, C.H. Hamilton and N. E. Paton (eds.), p.121, 1988.

[4] Z.X. Guo, J. P. Pilling and N. Ridley, "Bulge-Forming of Domes: A Comparison of Theoretical Prediction and Experiment," in Proceedings of an International Conference on SPF, C.H. Hamilton and N. E. Paton (eds.), p. 303, 1988.

[5] S.J. Hales, T.T. Bales, W.F. James, and J.M. Shinn, "Fabrication of Structural Components from Commercial Aluminum Alloys Using Superplastic Forming", in Superplasticity in Aerospace II, T.R. McNelley and H.C. Heikkenen (eds.), TMS-AIME, Warrendale, PA, 1990.

[6] F.W. Gayle, F.H. Heubaum, and J.R. Pickens, "Structure and Properties during Aging of an Ultra-High-Strength Al-Cu-Li-Ag-Mg Alloy", Scripta Metall., 24, p. 79, 1990.

[7] C.C Bampton, B.A. Cheney, A. Cho, A.K. Ghoch, and C. Gandhi, "Superplastic Forming of Al-Li Alloy 2090-QE16", in Proceedings of Superplasticity in Aerospace, p. 254, 1988.

[8] G.R. Martin, "Superplastic Formed Al-Li Aircraft Structure", AFWAL-TR-88-3080, p. 2-24, 1988.

[9] S.P. Agrawal and J.M. Truss, International Conference of Superplasticity in Aerospace-Aluminum, Cranfield, p. 296, 1985.

[10] H.C. Lipsius, J. Stock, and A. Shames, "Structural Evaluation of Superplastic Aluminum, Part I, Mechanical Corrosion, Metallurgical Data", AFWAL-TR-85-3050, 1985.

Report Documentation Page

1. Report No.	2. Government Accession No.	3. Recipient's Catalog No.
NASA CR-4367		

4. Title and Subtitle

Superplastic Formability of Al-Cu-Li Alloy Weldalite™ 049

5. Report Date

May 1991

6. Performing Organization Code

7. Author(s)

Bao-Tong (Bob) Ma
Joseph R. Pickens

8. Performing Organization Report No.

MML TR 90-47c

10. Work Unit No.

505-63-50-02

9. Performing Organization Name and Address

Martin Marietta Laboratories
1450 S. Rolling Road
Baltimore, MD 21227

11. Contract or Grant No.

NAS1-18531

13. Type of Report and Period Covered

Contractor Report

12. Sponsoring Agency Name and Address

National Aeronautics and Space Administration
Langley Research Center
Hampton, VA 23665-5225

14. Sponsoring Agency Code

15. Supplementary Notes

Langley Technical Monitor: William D. Brewer
Final Report - Part III

16. Abstract

Extensive research during the past decade shows that several aluminum lithium alloys can be processed to attain a microstructure that enables superplasticity. The high tensile strength of Al-Cu-Li alloy Weldalite™ 049 in the T4 and T6 tempers offers tremendous potential for attaining exceptional post-SPF properties. The SPF material used in this study is Weldalite™ 049 sheet that has been processed by Reynolds Metals Company's proprietary technique, which has been shown to induce SPF behavior in other Al-Cu-Li alloys. Martin Marietta Laboratories has evaluated the superplastic behavior and resulting post-SPF mechanical properties of this alloy, which was designed to be the next major structural alloy for space applications. The results indicate that Weldalite™ 049 alloy does indeed exhibit excellent superplasticity over wide range of temperatures and strain rates and excellent post-SPF tensile strength at various potential service temperatures.

17. Key Words (Suggested by Author(s))	18. Distribution Statement
Superplastic Formability	Unclassified - Unlimited Subject Category - 26

19. Security Classif. (of this report)	20. Security Classif. (of this page)	21. No. of pages	22. Price
Unclassified	Unclassified	79	A05

NASA FORM 1626 OCT 86

For sale by the National Technical Information Service, Springfield, Virginia 22161-2171

NASA-Langley, 1991